THE ABUNDANCES OF THE ELEMENTS IN G-TYPE SUBDWARFS*

LAWRENCE H. ALLER
University of Michigan Observatory
AND
JESSE L. GREENSTEIN
Mount Wilson and Palomar Observatories
Carnegie Institution of Washington, California Institute of Technology
Received January 25, 1960

ABSTRACT

High-dispersion spectroscopic analyses have been made of three G-type and one A-type subdwarfs. Because of the extreme weakness of the atomic lines, a large amount of observational material was collected for HD 19445 and HD 140283 (which has the highest weight); HD 219617, a star with intermediate line strengths has been treated less elaborately, as has been the high-velocity A star, HD 161817. A table of wave lengths and identifications is given in Table 2 for HD 19445; equivalent widths are given for the stronger lines in all stars in Table 3.

The weakness of ionized metals makes it difficult to determine the temperature spectroscopically. Consequently, we have based our temperatures on the U, B, V photoelectric colors or the scanning of the continuous spectra, with corrections for blanketing by the lines, made by Melbourne. Not all subdwarfs are identical in composition. The average deficiency of the metals, as compared with the sun, is by a factor of 40 in HD 19445, 100 in HD 140283, and 20 in HD 219617, while HD 161817 shows only small and uncertain deficiencies. The lines of CH were used to obtain an estimate of the carbon abundance, which was found to be very low in the G subdwarfs. There is some evidence for a greater than normal ratio of Ni/Fe. The mean relative abundances of the elements from C to Ba for the three G subdwarfs show some apparently real differences from solar values. We discuss the implications for theories of nucleogenesis. A rough analysis of the hydrogen-line profiles based on the Kolb-Griem theory of line broadening is satisfactory, except for an indication that the cores are superposed on broad, nearly undetectable wings.

INTRODUCTION

The subdwarfs of types F and G are the most extreme examples of population II near the sun. They have a low metal abundance, low rotation, high space velocity, and a distribution in space like that of the RR Lyrae stars. The designation "subdwarf" may be a misnomer, since they appear to fall near the main sequence in a color–absolute-magnitude array, if the colors are properly corrected for the blanketing effect of the metallic lines. Since few are bright, intensive spectroscopic studies may be carried out for only a small number of stars. Parallax data are poor. Miss Roman (1955) finds that their mean absolute magnitudes are +4 or +5 and their galactic orbits are highly eccentric and inclined.

The hydrogen lines appear to be of normal strength for late F stars and have sharp cores. The metallic lines are very weak and sharp. Their $B-V$ colors correspond to those of late F or G stars, but they are relatively bright in the ultraviolet. The blue and ultraviolet excesses are consequences of the fact that the normal F and G stars have a great number of metallic lines, increasing in both number and strength toward shorter wave lengths and depressing the continuum. The subdwarfs have lines (see below) as much as five times weaker than normal dwarfs.

Spectrograms of HD 19445 and HD 140283, secured by R. F. Sanford, were analyzed by Chamberlain and Aller (1951), who found that the character of the spectrum and the colors of these stars could be explained only by supposing that the hydrogen/metal

* This work was supported in part by the Air Force Office Scientific Research (ARDC) under contract AF 49(638)-21.

ratio was much larger than in the sun. Specifically they found that the abundances of iron and calcium were, respectively, about ten and thirty times lower than in the sun. More recently, the Burbidges (1956) determined the abundances of Mg, Al, Ca, Sc, Ti, Cr, Mn, Fe, Sr, Y, Zr, and Ba in five stars that were selected because they were believed to possess population II characteristics. For comparison, they used the same A0 star, 95 Leonis, as did Chamberlain and Aller. One of their stars, λ Bootis, appeared to have a composition similar to that of HD 19445 or HD 140283, while in 29 Cygni, HD 106223, and HD 161817 they found underabundance ratios intermediate between the extreme subdwarfs and normal stars. They also discussed the relations between chemical composition, space motion, and rotation.

If one adopts the point of view that elements are continuously being created in stars (Greenstein 1954; Fowler and Greenstein 1956; Burbidge, Burbidge, Fowler, and Hoyle 1957), the stars of very low metal-to-hydrogen ratio must represent a very old population. Hence it is of interest not only to find the mean underabundance factor for the metals but also to ascertain whether all metals are depleted by the same amount. Testing these hypotheses, important for theories of nucleogenesis, will require observations of the highest accuracy. The spectral lines are frequently very weak, and it is necessary to employ the largest attainable dispersions. We shall also see that it will be very difficult to obtain the temperature and that the temperature will play a decisive role in the absolute abundances.

OBSERVATIONAL DATA

The stars observed are listed in Table 1. The Mount Wilson plates for all were taken some years ago, and a first examination of the spectra was made then. The extreme sharpness and weakness of all lines, especially those of the ions and CH, made analysis difficult. We first carried out a complete study in 1955 of all four stars on the Mount Wilson plates, with results for HD 161817 and HD 219617 given in this paper. The stars HD 19445 and HD 140283 merited a more detailed investigation, and long exposures were then secured with the 200-inch coudé spectrograph at higher dispersion. The accuracy of equivalent widths for faint lines derived from the Palomar plates is at least twice that on the Mount Wilson plates. Consequently, the weighted means of the equivalent widths were obtained for HD 19445 and HD 140283, and the material was completely reanalyzed for these two important stars.

In order to provide a first summary of identifications and line intensities in a subdwarf, we have measured the Palomar spectrum, Pb 2345, and HD 19445 completely. Table 2 gives the measured data (supplemented in a very few instances by results from the Mount Wilson plates). The first three columns give the wave lengths, eye-estimates of intensity on an arbitrary scale, and the equivalent widths. We emphasize that these equivalent widths were measured (with few exceptions) on one plate only and are intended as a guide to identifications but *not* as the basis for a curve-of-growth analysis. (Table 3 lists the mean values of W to be used for theoretical discussions.) The fourth column of Table 2 gives the depression of the continuum for lines that fall on the wings of the Balmer lines or the K line. In each instance the equivalent width is measured with respect to the actual point in the hydrogen- or calcium-line profile where the line falls. Column 5 gives the suggested identifications. We list the laboratory wave length, the atom, ion, or molecule, and the multiplet number as given in Charlotte Moore Sitterly's *Revised Multiplet Table*. Notice that many of the lines are blended, even in a star with very weak lines.

In Table 3 are compiled the mean equivalent widths of the lines actually used in the curve-of-growth analyses. Both Mount Wilson and Palomar data were obtained for HD 19445 and HD 140283; these stars were emphasized in our work because the earlier studies had indicated that they probably represented the most extreme types of population II stars. HD 219617 and HD 161817 were observed only at Mount Wilson. The former is a close binary with moderately weak lines, whose components are of about equal brightness. The latter is a much hotter star, whose intrinsic luminosity is unknown, since its parallax is unreliable. Parenago (1958), on the basis of the U, B, V colors, concludes that it is a subluminous A5 star which falls near the RR Lyrae gap.

Babcock (1958) finds that HD 19445 has a magnetic field of the order of 1000 gauss. Unfortunately, no magnetic data are available for the other subdwarfs. In our curve-of-growth analysis we have neglected the influence of this magnetic field upon the broadening of the lines. As we shall see, no excess broadening is required by the empirical curve of growth.

TABLE 1

OBSERVATIONAL DATA

HD Object	1900 α	1900 δ	Plate*	Exposure (min.)	m_V	p	μ	Velocity† (km/sec)
19445......	3^h02^m5	+25°58′	Ce 6729	45	8.06	0″021±0″006	0″821	−139
			6743	120				
			8433	130				
			8440	100				
			Pb 2345	300				
140283.....	15 37.8	−10 37	Ce 7121	37	7.20	.031± .007	1.187	−171
			7241	25				
			9301	45				
			9343	180				
			Pb 1543	45				
			3176	273				
			4609	293				
161817‡....	17 42.6	+25 48	Ce 8429	50	6.98	....	0.055	−363
			8436	50				
219617§....	23 12.0	−14 27	Ce 8302	125	8.17	0.024±0.006	1.292	+ 10
			8306	108				

* The Mount Wilson coudé plates (Ce) are 10 A/mm and are somewhat narrow. The Palomar (Pb) plates are 4.5 A/mm and well widened.

† From R. E Wilson, *General Catalogue of Stellar Radial Velocities.*

‡ Miss Roman estimates $M = +2.5$.

§ ADS 16644; two nearly equal stars taken together.

ANALYSIS OF THE OBSERVATIONS

The main purposes of this investigation have been to provide, for a small sample of apparently metal-deficient stars, as accurate as possible observational data on identifications, equivalent widths, and profiles for the stronger lines. Accordingly, we shall not attempt an exhaustive theoretical discussion of the observational material. Such a program would require the use of model-atmosphere methods to take into account stratification effects in the calculation of equivalent widths, the representation of the hydrogen-line profiles, and the prediction of the energy distribution in the continuous spectrum. A network of model atmospheres requisite for such an analysis is not available, nor are the required masses, radii, or surface gravities known.

A curve-of-growth analysis would appear to be adequate for the purpose of a first reconnaissance. Accordingly, we have adopted Wrubel's (1949) curve of growth for pure scattering in the Milne-Eddington approximation. As ordinate, one employs

$$\log\left[\frac{W}{\lambda}\left(\frac{c}{v}\right)\right]$$

TABLE 2

LINES IN THE SPECTRUM OF

HD 19445 Pb 2345

(1) λ	(2) I	(3) EW	(4) °/o	(5) Identification
3758.25	0			8.24 FeI 21
59.28	0			9.29 TiII 13
60.05	0⁻d			0.05 FeI 177
60.54	0⁻			0.53 FeI 76
61.34	0			1.32 TiII 13
63.73	0⁻db			3.79 FeI 21
65.53	0⁻			5.59 FeI 608, 5.62 CrII 20
67.17	0			7.19 FeI 21
69.49	0			9.46 NiII 4
70.57				0.57 H
83.52	0			3.53 NiI 30
86.28	0⁻			6.18 FeI 367
86.67	0⁻			6.68 FeI 22
87.89	0			7.88 FeI 21
88.64	0			8.70 YII 7
90.12	On			0.10 FeI 22
95.04	0			5.00 FeI 21, 4.96 VI 28?
95.49	0⁻			5.54 FeI ⊙
97.76	ON			7.72 CrI (139)
97.90				7.10 H
98.16	0			CN?
98.55	0			8.51 FeI
99.99	0			9.81 TiII 13, 9.91 VI 28?
3805.32	0⁻			5.35 FeI 608?
06.19	0⁻			6.20 FeI 731
06.73	0⁻			6.70 FeI 607, 6.72 MnI 6
07.12	0			7.14 NiI 33
07.56	0⁻d			7.53 FeI 73
08.21	0⁻d			8.12 CeII 59?, FeI ⊙
08.75	Od			8.73 FeI 222
10.65	On			0.76 FeI 665
10.83	On			0.90 FeI 224
11.04	On			1.05 FeI 223, 287, CN? ⊙, 11.06 CoI 31
12.40	0⁻d			
12.99	1			2.96 FeI 22, 13.06 FeI 222
13.44	0⁻d			3.39 TiII 12, 3.49 VI 9
14.02	0⁻d			4.12 FeII 153, 3.89 FeI 854, 3.97 GdII 2
14.57	0			4.58 TiII 12, 4.53 FeI 22
15.07	0⁻d			
15.85	2			5.84 FeI 45

TABLE 2 (Continued)

LINES IN THE SPECTRUM OF

HD 19445 Pb 2345

(1) λ	(2) I	(3) EW	(4) •/⊙	(5) Identification
3816.35	0-d			6.39 FeI 73
20.44	2b			0.43 FeI 20
21.20	0-d			1.18 FeI 608
21.88	0			1.88 FeI
24.42	2			4.44 FeI 4
24.90	0-			4.91 FeII 29
25.31	0-			5.40 FeI 123, CN? ⊙
25.89	2			5.88 FeI 20
27.81	2			7.82 FeI 45
29.35	2-			9.35 MgI 3
29.81	0-			9.77 FeI 221
31.75	0-d			1.69 NiI 31?
32.33	3	.224	(10)	2.30 MgI 3
32.82	0-	.011	(12)	2.87 NiI 1, 2.89 YII 7
33.34	0-b	.017	(14)	3.31 FeI 221
34.21	1	.064	(18)	4.22 FeI 20
35.40	7			5.40 H
38.30	2b	.180	(7)	8.30 MgI 3
39.34	0	.019	(7)	9.26 FeI 529
39.81	0-	.014	(7)	9.78 MnI 6 ?
40.43	1	.086	(7)	0.44 FeI 20
40.71	0n	.017	(7)	0.75 VI 9, 0.72 LaII 28 ?
41.04	1	.064	(7)	1.05 FeI 45
42.16	0-bd	.016		CN ? ⊙
42.83	0n	.016		2.90 FeI 222
43.26	1	.057		3.26 FeI 528
44.15	0	.012		3.98 MnI 6, 4.28 NiI 137, CN ⊙
45.50	0-db	.059		5.47 CoI 34
46.37	0-d	.024		6.41 FeI 804
46.79	0-d	.040		6.80 FeI 664?
49.99	1	.096		9.97 FeI 20
50.87	0	.053		0.82 FeI 22, 0.97 GdII ?
51.25	0-			CN ⊙
52.18	0-	.014		2.10 VII 3, 2.22 CrI 24
52.59	0-	.033		2.57 FeI 73
56.38	1b	.109		6.37 FeI 4
57.26	0n	.030		
58.33	1	.080		8.30 NiI 32
59.22	1	.036		9.21 FeI 175, 9.24 MgI 21
59.95	2	.127		9.91 FeI 4
64.54	0?n	.011		CN ⊙
65.53	2	.084		5.53 FeI 20
65.96	0-	.016		CN ⊙
67.25	0d	.036		7.22 FeI 488
68.68	0-	.018		CN ⊙
70.93	0-d	.023		CN ⊙
71.82	0-	.040		1.75 FeI 429
72.51	2	.102		2.50 FeI 20
73.13	0	.067		3.12 CoI 18?
73.76	0-	.024		3.76 FeI 175

TABLE 2 (Continued)

LINES IN THE SPECTRUM OF

HD 19445 Pb 2345

(1) λ	(2) I	(3) EW	(4) •/•	(5) Identification
3874.04	0^-	.028		4.05 FeI 120, 3.95 CoI 18
76.00		.028		6.00 FeI
77.16	0^-	.025		CN ? ⊙
77.55	0^-	.012		CN ? ⊙
78.03	2	.101		8.02 FeI 20
78.64	3	.164		8.58 FeI 4, 8.66 FeI 175, 8.71 VII 33
84.33	0^-d	.017	(11)	4.36 FeI 282
85.52	0^-bd	.027	(14)	5.51 FeI 224
86.29	2	.114	(17)	6.28 FeI 4
86.55	0n	.010	(17)	6.59 VI 64 ?
87.07	2	.067	(22)	7.05 FeI 20
88.54	0d	.058	(40)	8.52 FeI 45
89.05	8			9.05 HI
92.88	0^-	.018	(6)	2.90 FeI 283, 2.98 FeI 567
94.05	0	.033	(4)	4.00 FeI 663, 4.07 CoI 34
95.65	1	.089	(4)	5.66 FeI 4
97.99	1	.075		8.01 FeI 20, 7.90 FeI 280
98.96	0^-	.007		9.04 FeI 175
99.14	0^-n	.005		9.14 VII 33
99.75	2	.094		9.71 FeI 4
3900.13	0	.006		0.18 VI 126?
00.55	2	.053		0.52 FeI 565, 0.55 TiII 34
00.85	0^-	.003		
01.10	0^-			
02.92	2	.093		2.95 FeI 45, 2.92 CrI 23
03.85	0	.027		3.77 ZrII 7, 3.91 FeI 429
04.47	0^-	.017		
05.52	2	.168		5.53 SiI 3
05.92	0^-	.016		5.89 NdII
06.47	1	.065		6.48 FeI 4
06.81	0^-	.007		6.75 FeI
07.91	0^-	.018		7.94 FeI 280
13.47	1	.059		3.46 TiII 34
14.30	0^-d	.026		4.33 VII 33, 4.27 FeI 567
15.64	0d?	.036		⊙
16.77	0d	.020		6.73 FeI 606
17.21	1	.046		7.19 FeI 20
18.24	0^-	.010		8.32 FeI 124
18.68	0	.026		8.64 FeI 430
19.12	0^-	.013		9.15 CrI 23
20.27	2	.077		0.26 FeI 4
22.91	2	.085		2.91 FeI 4
25.62	0^-	.028		5.65 FeI 364
26.00	0^-	.035		6.00 FeI, 562, 5.95 FeI 364
27.23	0^-	.023		
27.93	2	.110	(3)	7.92 FeI 4
28.13	0^-	.019	(3)	8.08 FeI 565
28.32	0	.019	(5)	8.28 SmII 17
30.29	2	.092	(15)	0.30 FeI 4
31.28	0n	.004	(25)	1.12 FeI 565
31.62	0^-	.004	(31)	

TABLE 2 (Continued)

LINES IN THE SPECTRUM OF

HD 19445 Pb 2345

(1) λ	(2) I	(3) EW	(4) %	(5) Identification
3933.66	15bb			3.66 CaII 1
36.55	0-	.008	(15)	
40.28	0-	.021	(3)	0.34 CeII 50
40.91	0	.038	(2)	0.89 FeI 20
41.25	0-	.014	(2)	1.28 FeI 562
41.58	0-	.014	(2)	1.51 NdII 27, 1.73 CoI 17, 1.49 CrI 23
41.94	0-	.008	(1)	1.92 ZrII 55
42.17	0-	.002		2.15 CeII 37
42.46	0	.012		2.44 FeI 364
43.98	2	.146		4.00 AlI 1
46.98	0-	.016		7.00 FeI 561
47.54	0-d	.015		7.53 FeI 361, 426
48.05	0-	.021		8.00 FeI 652, 8.10 FeI 562
48.45	On	.002		
48.70	1	.042		8.67 TiI, 8.78 FeI 604
49.03	0-	.007		9.14 FeI 730
49.38	0-	.011		
49.93	1	.030		9.95 FeI 72
50.43	0-	.015		0.35 YII 6
50.93	0-	.003		
51.14	0-d	.021		1.16 FeI 661
53.12	Odw	.016		3.16 FeI 430
56.40	0	.042		6.46 FeI 604, 6.34 TiI 13
56.68	0	.046		6.68 FeI 278
57.01	0	.017		7.03 FeI 562
58.18	0-	.025		8.21 TiI 13, 8.24 ZrII 16
58.69	0-d	.012		8.74 FeI RR T
59.69	0-	.009		
60.28	0-	.008		0.28 FeI 913
61.50	2	.094	(3)	1.52 AlI 1
62.86	On	.005	(5)	2.85 TiI 12
63.13	Od	.028	(6)	3.11 FeI 562
63.44	On	.004	(6)	
63.67	On	.011	(6)	3.69 CrI 38?, 3.62 VI
65.32	0	.015	(15)	
66.04	Od	.033	(20)	6.07 FeI 45
66.72	Od	.041	(29)	6.82 FeI 659, 6.63 FeI 282
67.97	4	.029	(69)	7.96 FeI 561
68.47	10bb			8.47 CaII 1
69.09	4	.027	(64)	9.26 FeI 43, 9.11 CoI
70.17	8bb			0.07 Hε
71.33	1	.012	(27)	1.33 FeI 277
73.59	1	.036	(11)	3.64 VII 9, 3.56 NiI 31
77.13	0-			7.18 CoI 113?
77.40	0-	.002	(3)	
77.72	1	.035	(2)	7.74 FeI 72
81.75	1	.028		1.76 TiI 12, 1.77 FeI 278
81.90	On	.013		

TABLE 2 (Continued)

LINES IN THE SPECTRUM OF

HD 19445 Pb 2345

(1) λ	(2) I	(3) EW	(4) °/°	(5) Identification
3983.61	0	.006		
83.96	1	.034		3.96 FeI 277
86.11	0	.019		6.18 FeI 655, 560
86.77	$\underline{0}$	.043		6.75 MgI 17, 6.83 MnI 33 ?
88.21	0^-	.009		
89.78	0^-d	.032		9.76 TiI 12
91.13	0^-	.017		1.14 ZrII 30, 1.12 CrI 38
91.65	0^-	.018		1.67 CrI 38, 1.68 CoI 17
92.18	0^-	.003		2.11 CrI 38
93.87	0^-	.012		3.82 CeII 12, 3.97 CrI 67
94.22	0^-	.013		4.12 FeI 526
94.85	0^-d	.009		4.83 PrII 11
95.32	$\underline{1}$	.035		5.31 CoI 31
95.73	0^-d	.067:		5.74 LaII 27
95.93		.130		6.00 FeI 279
96.95	0d			6.97 FeI 945
97.43	2	.046		7.39 FeI 278
98.03	1	.039		8.05 FeI 276
98.65	$\underline{1}$	.047		8.64 TiI 12, 8.73 VI 89
4001.69	0^-bd	.020		1.67 FeI 72
04.92	0n	.012		4.98, 4.83 FeI 601, 486, 557
05.26	2	.083		5.25 FeI 43
05.47	0n	.005		5.49 FeI ⊙
05.72	0	.011		5.71 VII 32
06.31	0	.002		6.31 FeI 603
06.58	$\underline{0}$	.013		6.63 FeI 488
08.55	0^-d	.009		
08.97	0^-d	.004		8.91 TiI 12?
09.73	1	.042		9.71 FeI 72, 9.65 TiI 11 ?
10.09	0	.006		0.18 FeI 915, 9.98 NiI 150?
10.55	$\underline{0}$	.008		0.77 FeI 219
11.43	0^-d	.003		1.41 FeI 218, 1.53 TiI 10 ?
11.72	0^-d	.002		1.71 FeI 153
12.10	0^-	.007		2.16 FeI 601 ?
12.43	$\underline{1}$	.057		2.37 TiII 11, 2.37 CeII 206, 2.47 FeII 126?
14.58	0^-d	.039		4.53 FeI 802, 4.49 ScII 8
15.24	0^-	.005		5.38 TiI 185?
15.64	0	.015		5.50 NiII 12
16.16	0	.002		6.26 TiI 186?
16.37	0	.018		6.43 FeI 560
17.18	0d	.022		7.10 FeI 279, 7.16 FeI 527, 7.29 VII 216?
17.57	$\underline{0}$	.006		7.56 NiI 171
18.24	0^-d	.015		8.28 FeI 560, 8.38 ZrII 54
18.95	0	.014		
20.35	0	.008		0.40 ScI 7?
21.89	2	.044		1.87 FeI 278, 1.81 TiI 185
24.73	0	.031		4.74 FeI 560

TABLE 2 (Continued)

LINES IN THE SPECTRUM OF

HD 19445 Pb 2345

(1) λ	(2) I	(3) EW	(4) •/•	(5) Identification
4025.16	0	.025		5.14 TiII 11
25.97	0	.008		5.87 LaII 42?, CH ⊙?
28.32	1	.021		8.33 TiII 87
28.83	0	.008		8.76 FeI ⊙
30.18	0	.008		0.19 FeI 72
30.44	0	.017		0.50 FeI 560, 0.51 TiI 185
30.76	2	.074		0.76 MnI 2
31.77	0	.007		1.68 LaII 40, 1.97 FeI 655
33.10	2	.057		3.07 MnI 2
33.52	0^-d	.004		
34.52	2	.067		4.49 MnI 2
35.74	0^-	.017		5.74 MnI 2, 5.63 VII 32
40.71	0^-d	.019		0.65 FeI 655
43.93	0^-d	.014		3.90 FeI 276, 557
44.60	0^-	.030		4.61 FeI 359
45.82	4	.157		5.81 FeI 43
46.22	0	.013		6.27 VII 177
46.58	0	.007		6.63 FeI 487
53.28	0	.010		3.27 FeI ⊙
53.84	0	.016		3.81 TiII 87, 3.82 FeI 485
55.98	0	.009		5.98 FeI 914
56.56	0^-	.006		6.53 FeI 320
57.08	0^-	.005		7.07 VI 121
57.36	0	.015		7.36 FeI 277
57.52	1	.033		7.46 FeII 212, 7.50 MgI 16
57.86	0	.010		7.95 MnI 29, 7.81 Pb 1, 7.81 CrI 251?
58.16	0	.011		
62.47	0	.035		2.47 FeI 359
62.72	0^-			
63.23	0^-			3.29 FeI 698
63.61	4			3.60 FeI 43
65.12	0			5.09 TiI 80
65.36	0	.012		5.40 FeI 698
66.33	0	.007		6.36 CoI 30
66.59	0^-	.007		6.60 FeI 424
67.01	0	.023		6.98 FeI 358
67.31	0d	.007		7.28 FeI 217
67.57	0^-	.006		
67.97	1	.029		7.98 FeI 559
71.75	4	.120		1.74 FeI 43
73.79	0	.012		3.76 FeI 558
74.78	0	.012		4.79 FeI 524
76.64	0d	.038		6.69 FeI 558
77.74	4	.098		7.71 SrII 1
78.18	0^-	.002		8.32 CeII 19
78.40	0^-	.021		8.47 TiI 80, 8.36 FeI 217
80.20	0^-	.007		0.23 FeI 558
84.54	0	.035		4.50 FeI 698
85.00	0	.008		5.01 FeI 358
85.34	0	.018		5.31 FeI 559

TABLE 2 (Continued)

LINES IN THE SPECTRUM OF

HD 19445 Pb 2345

(1) λ	(2) I	(3) EW	(4) °/o	(5) Identification
4087.22	0			7.10 FeI 694
87.51	0			7.63 CrII 19?
90.45	0	.006		0.52 ZrII 29, 0.34 Fe, Cr ⊙
94.14	0̲	.005	(3)	
95.99	0⁻	.016	(5)	5.98 FeI 217
98.20	0	.014	(10)	8.18 FeI 558
98.51	0	.012	(10)	8.53 CaI 25
4100.55	0	.010	(26)	
00.79	0	.008	(30)	0.74 FeI 18
01.65	10			1.74 Hδ
02.61	0			
02.94	1	.020	(26)	2.93 SiI 2
07.49	1	.016	(7)	7.49 FeI 354
12.29		.003	(3)	2.35 FeI 695
12.65	:	.006		2.71 TiI 9
12.88	:	.005		2.97 FeI 1103?
13.18	0	.005		3.21 ZnI ?
14.46	0	.010		4.45 FeI 357
14.72	0	.005		
16.92	0	.004		6.97 FeI 558
18.30	0bd	.005		8.18 VI 112, 8.14 CeII 11
18.54	1	.035		8.55 FeI 801
18.85	0	.016		8.90 FeI 559, 8.77 CoI 28
20.16	0	.012		0.21 FeI 423
21.31	2	.028		1.32 CoI 28
21.84	0	.007		1.81 FeI 356
22.15	0	.005		2.14 TiI 296, 2.16 CrI 65
22.52	0	.008		2.64 FeII 28, 2.52 FeI 356
22.72	-	.003		2.76 MnI 47 ?
25.25	0̲⁻	.004		5.23 FeI 173P, ⊙
25.59	0̲⁻	.004		5.62 FeI 1103
25.90	0⁻	.006		5.88 FeI 354
26.21	0	.009		6.19 FeI 695
26.42	0	.004		6.52 CrI 35
26.96	0	.005		6.88 FeI 354
27.60	0̲	.019		7.61 FeI 357
27.89	0⁻	.005		7.81 FeI, 558, 727
28.33	0			8.31 YII 5
29.13				
29.44				9.46 FeI 695
29.74				9.73 Eu II 1
32.07	3	.085		2.06 FeI 43
32.53	0	.005		2.54 FeI 1103, 2.50 LaII 50?
32.93	0d	.018		2.94, 2.90 FeI 357
33.45				3.36 NdII 19 ?
33.80	0	.006		3.87 FeI 698, 3.80 CeII 4
34.26	0̲			4.34 FeI 3
34.47	0⁻			4.43 FeI 482, 697

TABLE 2 (Continued)

LINES IN THE SPECTRUM OF

HD 19445 Pb 2345

(1) λ	(2) I	(3) EW	(4) °/o	(5) Identification
4134.70	$\underline{1}$	.027		4.68 FeI 357
34.96	0^-			
35.14	0^-			
35.31	$\underline{0}$	.007		5.33 NdII, ⊙
37.02	0^-	.010		7.00 FeI 726
37.86	0^-	.002		7.97 FeI 320, 7.65 CeII 2
38.34	0^-	.002		
39.87	0^-	.004		9.93 FeI 18
41.84	0^-	.006		1.86 FeI 422
42.13	0^-	.002		2.18 NiI 212?, 2.19 CrI 305?
42.32	0^-	.005		2.38 CrII 31
42.97	0			
43.41	3	.037		3.41 FeI 523
43.87	5	.076		3.87 FeI 43
45.37	0^-	.001		5.21 FeI 274?
45.66	0^-	.005		5.77 CrI 162?
46.03	0^-	.004		6.07 FeI 422
46.68	0^-	.002		6.70 CrI 107?
46.84	0^-			
47.51	0			7.53 MnI 37?
47.69	$\underline{0}$			7.67 FeI 42
49.27	0^-	.008		9.22 ZrII 41
49.67	0^-			9.76 FeI 3P, ⊙
50.30	0^-d	.003		0.26 FeI 695
51.06	0^-d	.007		0.97 ZrII 42
51.83	0^-	.009		1.96 FeI 764, 1.98 LaII 40
52.17	0^-	.012		2.17 FeI 18
52.55	0^-			2.39, 2.53 CN ⊙
52.76	0^-			2.78 CrI 261, 2.78 LaII 78
53.04	0			3.07 CrI 35
53.88	0	.023		3.91 FeI 695, 3.81 CrI ⊙
54.52	0	.026		4.50 FeI 355
54.82	0	.024		4.81 FeI 694
55.27	$\underline{0}$	.005		5.22 SmII bl 8 ?
55.86	0^-	.004		
56.19	$\underline{0}$	.009		6.24 ZrII 29
56.33	0^-			6.31 ⊙
56.79	0	.025		6.80 FeI 354
57.18	0	.011		
57.61	0	.025		
57.80	0			7.79 FeI 695
64.19	0	.008		1.13 TiI 163?, 4.19 PrII 8, 4.24 Fe 694
64.52	0	.004		4.52 CN ⊙?
67.27	3	.047		7.27 MgI 15
70.08	0	.004		0.15 CN ⊙?
70.39	0			0.35 CN ⊙?
70.93	0	.021		0.91 FeI 482
71.69	0	.010		1.70 FeI 941
71.90	0	.020		1.90 FeI 650, 1.90 TiII 105

TABLE 2 (Continued)

LINES IN THE SPECTRUM OF

HD 19445 Pb 2345

(1) λ	(2) I	(3) EW	(4) °/o	(5) Identification
4172.15	0	.011		2.13 FeI 649
72.69	0	.016		2.69 CrII 18, 2.75 FeI 19
73.11	0^-			3.68 FeI 698
73.45	0	.025		3.45 FeII 27, 3.54 TiII
73.69	0^-	.004		3.76 YII 23, CN ⊙ bl
74.00	0^-	.007		3.93 FeI 19
74.31	0	.001		4.32 CN ⊙?
74.97	0^-d	.006		4.92 FeI 19
75.66	1	.030		5.64 FeI 354
76.34	0^-			bl CN ⊙
76.62	0	.019		6.57 FeI 695
77.38	0^-n	.004		7.36 TiI 163?, 7.32 NdII 10
77.57	0d	.017		7.60 FeI 18, 7.54 YII 14
77.83	0n	.008		7.85 CN ⊙?
78.67	0^-d	.002		CN ⊙?
78.83	1	.018		8.86 FeII 28
79.78	0	.004		9.81 ZrII 99
80.17	0	.005		bl CN ⊙
81.78	3	.046		1.76 FeI 354
82.32	0^-			2.38 FeI 476a
83.42	0^-d	.012		3.43 VII 37
84.93	0^-b	.021		4.90 FeI 355, 4.90 CrI 155
87.05	4	.055		7.04 FeI 152
87.47	0^-			7.59 FeI 694
87.81	3d	.060		7.80 FeI 152
88.42	0^-			
88.76	0^-	.006		8.69 TiI 220?, ⊙?
91.30	0^-	.049		1.27 CrI 35
91.43	1			1.43 FeI 152
95.34	0^-d	.038		5.34 FeI 693
96.21	0	.011		6.22 FeI 693
96.60	0	.004		6.55 LaII 41, 6.53 FeI 418
98.29	4	.063		8.31 FeI 152, 8.27 693
98.65	0	.018		8.65 FeI 693
99.11	3	.063		9.10 FeI 522
4200.95	0^-	.014		0.93 FeI 689
02.03	5	.075		2.03 FeI 42
03.99	0^-d	.028		3.95 FeI 850, 3.99 FeI 355
04.76	0^-d	.014		4.69 YII 1, 4.76 CH ⊙
05.51	0^-d	.013		5.55 FeI 689
06.45	0^-	.002		6.38 MnII 7 ?
06.68	1	.019		6.70 FeI 3
08.64	0d	.022		8.61 FeI 689, 696
09.85	0^-d	.004		9.86 VI 24
10.38	2	.045		0.35 FeI 152
10.93	0	.008		0.77 CrI 106, 0.97 CH ⊙
11.91	0	.012		1.88 ZrII 15
12.63	0d	.027		2.64 Cr ⊙ ?
13.67	0d	.027		3.65 FeI 355, CN, CH bl ⊙
13.93	0^-s	.009		3.91 CN ⊙ ?

TABLE 2 (Continued)

LINES IN THE SPECTRUM OF

HD 19445 Pb 2345

(1) λ	(2) I	(3) EW	(4) $^{o}/o$	(5) Identification
4214.46	0d	.006		bl CN ⊙ ?
15.21	0	.003		bl CN ⊙ ?
15.53	4	.084		5.52 SrII 1, CN ⊙ ?
15.91	0	.006		5.98 FeI 273, CN ⊙
16.19	1	.035		6.19 FeI 3
17.60	0	.017		7.63 CrI 132, 7.55 Fe 693, 7.56 LaII 78
18.50	0d			
18.83	0d	.026		8.73 CH ⊙, 8.71 VI 24?
19.06	0-			
19.39	2	.037		9.36 FeI 800
19.68	0-d	.011		9.59 FeI 763, 9.74 FeI 832?
20.70	0-	.006		0.70 SmII 15, 50
21.05	0-	.008		
22.19	2	.031		2.22 FeI 152
23.50	0-bd	.019		3.49 CH ⊙
24.16	0b	.034		4.18 FeI 689
24.54	0-d	.010		4.51 CrI 155, 4.51 FeI 689
24.84	0-d	.016		4.86 CH ⊙
25.45	0d	.015		5.46 FeI 693
26.02	0	.006		5.96 FeI 521
26.75	6	.234		6.72 CaI 2
27.12	0	.009		
27.44	2	.050		7.43 FeI 693
30.98	0-	.024		0.95 LaII 83, 1.03 CH ⊙
33.17	3	.034		3.17 FeII 27
33.62	3	.051		3.61 FeI 152
35.93	4	.075		5.94 FeI 152
38.05	0-d	.019		8.03 FeI 689, 696
38.82	0	.025		8.82 FeI 693
42.02	0-bd	.015		
42.25	0-bd	.004		
42.38	0-bd	.011		2.38 CrII 31, bl CH ⊙
46.42	0	.002		
46.84	3	.059		6.83 ScII 7
47.42	2	.024		7.43 FeI 693
47.60	0	.003		
49.58	0-d	.018		bl CH ⊙
50.13	4	.058		0.13 FeI 152
50.80	4	.068		0.79 FeI 42
54.35	4	.068		4.35 CrI 1
59.81	0-			
60.49	6	.087		0.48 FeI 152
65.46	0-	.015		
65.72	0-	.003		5.72 TiI 162 ?
66.53	0-	.008		
67.01	0-d	.018		6.99 FeI 273
67.37	0	.012		7.39 CH ⊙
67.80	0	.034		7.83 FeI 482
68.17	0-	.010		
71.17	4	.061		1.16 FeI 152

TABLE 2 (Continued)

LINES IN THE SPECTRUM OF

HD 19445 Pb 2345

(1) λ	(2) I	(3) EW	(4) °/o	(5) Identification
4271.77	6	.094		1.76 FeI 42
74.81	5	.053		4.80 CrI 1
79.77	0^-	.018		9.86 FeI 351, 9.72 CH ⊙
80.05	0^-	.013		0.07 TiI 252?, bl CH ⊙
81.96	0^-	.007		1.97 CH ⊙
82.41	3	.042		2.41 FeI 71
83.00	2	.056		3.01 CaI 5
84.18	0^-	.015		4.21 CrII 31
84.70	0^-	.009		4.73 CrI 96, 4.84 CH ⊙
85.44	0^-d	.026		5.44 FeI 597
86.07	0^-	.017		6.00 TiI 44, bl CH ⊙
86.49	0^-	.026		6.44 FeI 414, CH ⊙
86.94	0^-d			6.98 FeI 976, 6.97 LaII 75
87.90	0^-d	.006		7.90 TiII 20?
88.70	0	.015		8.78 VII 17
89.02	0^-	.022		8.96 FeI 214, 9.07 TiI 44
89.35	1	.031		9.36 CaI 5
89.71	2	.064		9.72 CrI 1
90.22	2	.045		0.22 TiII
90.91	0	.019		0.87 FeI 351, 0.93 TiI 44
91.14	0	.020		1.21 TiI 45, 147
91.49	0^-	.011		1.47 FeI 3, 41
92.00	0^-d	.033		1.96 CrI 240, 2.05 CH ⊙
93.09	0bd	.037		3.12 CH ⊙
94.12	4	.071		4.13 FeI 41, 4.10 TiII 20
95.18	0bd	.033		bl CH ⊙
96.64	0d	.021		6.57 FeII 28
97.01	0^-	.016		7.05 CrI 64, 6.96 CH ⊙
97.24	0^-	.019		7.21 CH ⊙
97.54	0^-	.013		7.53 CH ⊙, 7.60 BaII 7?
97.98	0	.016		8.04 FeI 520, 7.98 CH ⊙?
98.77	0	.018		8.77 NiI 28, 8.82 CH ⊙, 8.66 TiI 44
99.00	0	.028		8.99 CaI 5
99.24	2	.065		9.24 FeI 152, 9.23 TiI 148
99.58	0^-d	.003		9.64 TiI 43, 9.65 FeI 416
4300.06	2	.070		0.05 TiII 41
00.59	0d	.036		0.57 TiII 44, CH ⊙ ?
00.86	0^-	.008		0.83 FeI 976, 1.00 CH ⊙
01.10	0d	.037		1.09 TiI 44, bl CH ⊙
01.90	0d	.024		1.93 TiII 41
02.28	0	.020		2.19 FeI 520, bl CH ⊙
02.54	2	.062		2.53 CaI 5
03.13	0	.022		3.13 FeII
03.91	0d	.037		bl CH ⊙
04.44	0^-d	.021		4.55 FeI 414, bl CH ⊙
05.36	0^-	.026		bl CH ⊙
05.66	0	.013		5.71 ScII 15
05.91	1d	.044		5.91 TiI 44

TABLE 2 (Continued)

LINES IN THE SPECTRUM OF

HD 19445 Pb 2345

(1) λ	(2) I	(3) EW	(4) °/o	(5) Identification
4306.15	0	.018		6.21 YI 5, 6.15 CH ⊙
06.78	0d	.039		bl CH ⊙
07.51	0	.018	(6)	bl CH ⊙
07.89	6	.160		7.90 FeI 42, 7.90 TiII 41, 7.74 CaI 5
08.24	0s	.012	(6)	8.18 CH ⊙
08.61	0-s	.012		
08.94	0-d	.015		8.94 ZrII 88?, 9.04 FeI 849
09.37	0-	.034		9.38 FeI 414
10.14	0-d	.022		bl CH ⊙
12.21	0-d	.018		2.23 ZrII 99, 2.09 CH ⊙
12.58	0-	.004		2.55 MnI 23
12.89	2	.060		2.86 TiII 41, bl CH ⊙
13.65	0	.008		3.63 CH ⊙
14.11	1	.039		4.08 ScII 15
15.05	2	.089		5.09 FeI 71, 4.98 TiII 41
18.14	0	.014		
18.64	2	.048		8.65 CaI 5
20.76	0bd	.034		0.75 ScII 15
20.98	0-	.013		0.98 TiII 41
23.23	0	.021		3.23 CH
25.76	5	.125		5.77 FeI 42
37.07	2	.039	(11)	7.05 FeI 41
37.55	0	.014	(14)	7.57 CrI 22
37.90	2	.049	(16)	7.92 TiII 20
38.35	0_	.009	(19)	8.26 FeI 70
38.85	0-	.011	(22)	8.84 FeI 117?, 8.80 CrI 198
40.49	12bb			0.47 Hγ
44.52	0	.015	(11)	4.51 CrI 22
51.85	3bd	.110		1.89 MgI 14
52.74	1	.060		2.74 FeI 71
60.46	0	.014		0.49 TiI 204, 0.46 CH ⊙
67.62	0	.032		7.58 FeI 414, 7.66 TiII 104
69.35	0-			9.41 FeII 28
69.76	0			9.77 FeI 518
70.98	0	.011		0.96 ZrII 79
71.26	0_	.009		1.28 CrI 22
71.92	0_	.006		
72.11	0-	.003		
72.84	0bd	.018		2.99 FeI 473, 2.74 CH ⊙ ?
74.45	0	.028		4.46 ScII 14, 4.50 FeI 648
74.95	0_	.015		4.94 YII 13
75.62	0-	.014		bl CH ⊙ ?
75.94	2	.060		5.93 FeI 2
76.29	0-	.010		
76.60	0-	.010		6.78 FeI 471, 904, 6.80 CrI 304
77.29	0bbd	.010		7.33 FeI 990, 7.24 CH ⊙
83.58	b	.175		3.55 FeI 41
90.50	0-	.012		0.46 FeI 413

TABLE 2 (Continued)

LINES IN THE SPECTRUM OF

HD 19445 Pb 2345

(1) λ	(2) I	(3) EW	(4) °/o	(5) Identification
4391.03	0⁻	.014		0.98 TiII 61, 0.95 FeI 414
93.65	0⁻	.014		3.53 CrI 102
94.07	0⁻b	.023		4.07 TiII 51
95.05	3	.076		5.03 TiII 19
95.28	0	.012		5.29 FeI 828
99.80	1	.044		9.77 TiII 51, 9.82 CrI 129
4400.44	0	.018		0.36 ScII 14
01.55	0	.027		1.55 NiI 86, 1.48 FeI 350
04.76	5	.129		4.75 FeI 41
07.65	0⁻d	.018		7.65 VI 22?, 7.68 TiII 51
08.48	0	.026		8.42 FeI 68, 8.51 VI 22
15.13	3	.083		5.13 FeI 41
15.56	0	.013		5.56 ScII
16.83	0⁻	.007		6.83 FeII
17.71	1	.050		7.71 TiII 40
22.57	0	.029		2.57 FeI 350, 2.59 YII 5
25.44	1	.040		5.44 CaI 4
26.41	0			
26.90	0	.010		7.10 TiI 128 ??
27.32	2	.055		7.31 FeI 2
30.66	0	.024		0.62 FeI 68
34.95	2	.057		4.96 CaI 4
35.66	1	.034		5.69 CaI 4
41.50	0	.010		
41.91	0⁻	.002		Fe ⊙ ?
42.35	1d	.043		2.34 FeI 68
42.68	0⁻	.006		
43.16	0bd	.026		3.20 FeI 350
43.79	1	.049		3.80 TiII 19
44.63	0⁻	.009		4.56 TiII 31
46.80	0⁻	.010		6.84 FeI 828
47.71	2	.032		7.72 FeI 68
49.16	0⁻	.011		9.14 TiI 160
50.49	0⁻	.023		0.49 TiII 19
54.33	0⁻	.011		4.38 FeI 350
54.80	3	.064		4.78 CaI 4
55.33	0⁻	.009		5.32 MnI 28, 5.32 TiI 113
55.92	1	.034		5.87 CaI 4
59.12	1	.042		9.12 FeI 68
61.66	2	.049		1.65 FeI 2
64.44	0⁻	.018		4.46 TiII 20
65.19	0⁻			5.19 CrI 267
66.56	1	.038		6.55 FeI 350
68.51	2	.053		8.49 TiII 31
69.42	0d	.025		9.38 FeI 830
75.64	0⁻	.004		5.70 VII 199
76.02	1	.036		6.02 FeI 350, 6.08 FeI 83
81.14	0⁻d	.023		1.28 TiII 146, 1.13 MgII 4

TABLE 2 (Continued)

LINES IN THE SPECTRUM OF

HD 19445 Pb 2345

(1) λ	(2) I	(3) EW	(4) °/o	(5) Identification
4481.88	0⁻	.006		
82.22	2b	.054		2.17 FeI 2, 2.26 FeI 68
84.25	0	.006		4.23 FeI 828
85.37	0⁻	.002		5.44 ZrII 79?
88.28	0	.006		8.32 TiII 115, 8.14 FeI 819
94.58	2	.039		4.57 FeI 68
4501.27	3	.050		1.27 TiII 31
08.30	0	.017		8.23 FeII 38
15.29	0	.019		5.34 FeII 37
20.26	0	.014		0.23 FeII 37
21.16	0	.009		1.14 CrI 277, 287?
22.69	0d	.019		2.80 TiI 42, 2.63 FeII 38
27.28	0	.005		7.30 TiI 42
28.64	2	.050		8.62 FeI 68
28.95	0	.009		
30.23	0	.009		
31.18	0d	.022		1.15 FeI 39
32.44	0	.009		
33.24	0	.030		3.24 TiI 42
33.99	3	.064		3.97 TiII 50
34.81	0bd	.021		4.78 TiI 42
35.93	0	.031		5.93 TiI bl
49.59	4b	.089		9.62 TiII 82, 9.97 FeII 38
54.06	2w	.055		4.03 BaII 1
55.92	0	.031		5.89 FeII 37
58.65	0	.017		8.65 CrII
63.22	0			3.24 CrI 246?
63.75	2	.058		3.76 TiII 50
71.10	2	.053		1.10 MgI
71.99	2	.060		1.97 TiII 82
72.45	0			
76.34	0	.037		6.34 FeII
78.56	0	.008		8.56 CaI
83.03	0	.011		2.94 FeI 348
83.85	2	.028		3.83 FeII 38
84.88	0	.015		4.82 FeI 822
85.83	0	.026		5.87 CaI 23
4600.69	0	.008		0.75 CrI 21
02.95	1	.051		2.94 FeI 39
99.36	0			⊙ ?
4705.30	2			5.46 FeI 752
18.34	0			8.43 CrI 186
36.11	0			6.13 CrI 195
36.75	0d			6.78 FeI 554
4861.33	10bd			1.33 Hβ
70.08	0d			0.13 TiI 231
70.78	0			0.81 CrI 143
71.37	0			1.32 FeI 318
71.76	0			
72.18	0d			2.14 FeI 318

TABLE 2 (Continued)

LINES IN THE SPECTRUM OF

HD 19445 Pb 2345

(1) λ	(2) I	(3) EW	(4) °/o	(5) Identification
4874.45	0			
74.81	0			4.81 VII 197 ?
78.08	0d			8.13 CaI 35
90.75	0			0.76 FeI 318
90.96	0			
91.56	0			1.50 FeI 318
4920.54	0d			0.51 FeI 318
21.78	0-			1.77 TiI 200
23.93	0			3.92 FeII 42

TABLE 3

EQUIVALENT WIDTHS OF LINES IN SUBDWARFS

Units, milliangstroms

λ	Ident.	HD 219617	HD 140283	HD 19445	HD 161817	Back-ground HD161817	Identifications -log $^W/\lambda$ ⊙
3651.85	Fe,ScII	.083	-	-	-		4.27 FeI
70.43	Ni	.075	-	-	-		4.46 NiI
79.92	Fe	-	.088	-	-		3.82 FeI
85.20	TiII	.104	.103	-	-		4.01 TiII
94.03	Fe	-	.038	-	-		4.37 FeI
3703.	H	.176	-	.190	-		
06.0	CaII	-	.123:	-	-		
09.31	Fe	.106	.091	.068	-		3.73 FeI
11.	H	.287	-	.330	-		
19.96	Fe	.294	.156	.178	-		3.20 FeI
22.	H	.480	-	.480	-		
24.40	Fe	.059	.041	.037	-		4.28 FeI
27.67	Fe	.153	.118	.139	-		3.80 FeI
35.	H	.765	-	.800	-		
37.06	Fe CaII bl	.287	.105: .073:	.270	-		3.30 FeI
44.09	Fe	.054	.024	.022	-		4.55 FeI
45.58	Fe	.174	.123	.157	-		3.45 FeI
45.91	Fe	.155	.106	.110	-		3.58 FeI
58.24	Fe	.22	.131	.130	.123		3.41 FeI
59.29	TiII	.156	.097	.105	.161		3.97 TiII
60.05	Fe	.051	.030:	-	.019		4.44 FeI
60.54	Fe	.038	.018:	-	-		4.56 FeI

TABLE 3 (Continued)

λ	Ident.	HD 219617	HD 140283	HD 19445	HD 161817	Back-ground HD161817	Identifications −log W/λ ⊙
3763.81	Fe	.216	.124	.128	.094	90°/o	3.65 FeI
70.57	H	.735	-	-	-		
75.55	Ni	.045	.053	.040	-		4.35 NiI
83.52	Ni	.055	.066	.047	.093		4.32 NiI
87.89	Fe	.076	.084	.062	.061	94°/o	3.78 FeI
90.10	Fe	.054	.065	.055	.032	88°/o	4.21 FeI
3805.35	Fe	.070	.047	-	-		4.33 FeI
07.14	Ni	.084	.066	.065	.025	86°/o	4.49 NiI
07.53	Fe	.055	.016	-	-		4.27 FeI
10.70	Fe bl	.030	-	-	.023	95°/o	
11.90	Fe	.033	-	-	.016	97°/o	
13.0	Fe bl	-	.089	-	-		
13.40	TiII	-	.015	-	-		
15.84	Fe	.235	.112	.127	.095		3.42 FeI
20.43	Fe	.290	.148	.183	.129		3.26 FeI
21.18	Fe	.086	.031	.023	.039		4.59 FeI
21.88	Fe	.055	.019	.024	.050		4.63 FeI
25.88	Fe	.298	.125	.165	.110	85°/o	3.33 FeI
27.82	Fe	.183	.089	.130	.145		3.65 FeI
29.35	Mg	.267	.111	.183	.102	77°/o	3.94 MgI
32.30	Mg	.320	.145	.208	.151	60°/o	3.66 MgI
38.30	Mg	.385	.165	.248:	.141	56°/o	3.57 MgI
49.97	Fe	.122	.088	.085	.075	96°/o	3.74 FeI
50.82	Fe	.071	.049	.041	.039:		4.17 FeI
52.57	Fe	.043	.022	.032	.031		4.44 FeI
56.37	Fe	.138	.094	.101	.147		3.61 FeI

TABLE 3 (Continued)

λ	Ident.	HD 219617	HD 140283	HD 19445	HD 161817	Back-ground HD161817	Identifications -log W/λ ⊙
3858.30	Ni	.083	.060	.071	.046		4.31 NiI
59.21	Fe	.062	.011	.029	.030		4.64 FeI
59.91	Fe	.272	.135	.156	.093		3.46 FeI
65.53	Fe	.110	.059	.077	.071		3.89 FeI
67.22	Fe	.063	.018	.036:	-		4.50 FeI
73.12	Co	.063	.041	.074	.025	92°/o	4.56 FeI
76.00	Fe	.052	.014	.028	.022		4.39 FeI
78.02	Fe	.139	.081	.089	.039	84°/o	3.80 FeI
78.58	Fe	.215	.123	.149	.035	83°/o	3.68 ? FeI
86.28	Fe	.161	.110	.094	.092	54°/o	3.51 FeI
95.66	Fe	.150	.091	.088	.042	71°/o	3.88 FeI
99.71	Fe	.117	.085	.087	.070	83°/o	3.82 FeI
3902.95	Fe,Cr	.129	.077	.095	.065	90°/o	3.73 FeI
05.53	Si	.258	.112	.171	.076	94°/o	3.65 SiI
06.48	Fe	.106	.068	.069	.069:	95°/o	4.14 FeI
17.19	Fe	.060	.036	.046	-		4.27 FeI
20.26	Fe	.106	.079	.080	.075		3.86 FeI
22.91	Fe	.140	.089	.090	.071:		3.99 FeI
30.30	Fe	.088	.092	.089	.061	99°/o	3.89 FeI
44.00	Al	.145	.080	.138	.098		3.56 AlI
61.52	Al	.123	.069	.089	.067	78°/o	3.67 AlI
86.75	Mg,Mn	.076	.011	.035	-		4.18 MgI
98.64	Ti	.049	.022	.040	.016		4.44 TiI
4005.25	Fe	.138	.077	.077	.070		3.93 FeI
12.37	CeII,TiII	.062	.038	.042	.047		4.56 FeI
25.14	TiII	.048	.018	.022	.047		4.53 TiII

TABLE 3 (Continued)

λ	Ident.	HD 219617	HD 140283	HD 19445	HD 161817	Back-ground HD161817	Identifications -log W/λ ⊙
4028.33	TiII	.032	.020	.020	.053		4.58 TiII
33.07	Mn	.087	.050	.060	.013		4.13 MnI
34.49	Mn	.081	.046	.082	.012		4.24 MnI
35.74	VII,Mn	.030	.013	.017	-		4.74 VII 4.49 MnI
45.81	Fe	.274	.133	.164	.137		3.47 FeI
63.60	Fe	.200	.098	.117	.109		3.65 FeI
71.74	Fe	.166	.091	.103	.090		3.66 FeI
77.71	SrII	.117	.075	.085	.167		3.98 SrII
4111.79	V	.018	.004:	-	-		4.50 VI
32.06	Fe	.128	.077	.088	.048		3.95 FeI
43.87	Fe	.110	.076	.081	.043		3.91 FeI
67.27	Mg	.086	.028	.069	.032		4.13 MgI
72.69	Fe,CrII	.046	.017	.016	.016		4.61 FeI
78.86	FeII	.043	.015	.018	.035		4.62 FeII
4202.03	Fe	.10	.075	.072	.053		3.93 FeI
06.70	Fe	.038	.018	.019:	.014		4.57 FeI
15.52	SrII	.128	.055	.085	.084		4.19 SrII
16.19	Fe	.045	.034	.037	.020:		4.53 FeI
18.81	CH	.112	.006:	.026:	-		4.73 CH
22.22	Fe	.057	.025	.038	.020:		4.30 FeI
23.48	CH	-	.018	-	-		
26.72	Ca	.452	.130	.199	.136		3.45 CaI
27.43	Fe	.033	.031	.049	.039		4.19 FeI
33.17	FeII	.057	.036	.031	.100		4.47 FeII
33.61	Fe	.052	.033	.040	.021		4.14 FeI
38.82	Fe	.042	.017	.025:	.010		4.35 FeI
46.83	ScII	.068	.041	.054	.094		4.36 ScII

TABLE 3 (Continued)

λ	Ident.	HD 219617	HD 140283	HD 19445	HD 161817	Back-ground HD161817	Identifications -log W/λ ⊙
4249.64	CH	-	.014	-	-		
50.13	Fe	.075	.041	.058	.021		3.98 FeI
50.79	Fe	.081	.068	.061	.051		3.96 FeI
54.35	Cr	.078	.054	.076	.026		3.97 CrI
60.48	Fe	.141	.072	.072	.057		3.78 FeI
64.21	Fe	.017	-	-	.028		4.77 FeI
66.99	Fe	.010	-	.018:	-		4.69 FeI
67.39	CH	-	.008	-	-		
71.16	Fe	.081	.042	.064	.035		3.97 FeI
71.76	Fe	.152	.083	.101	.075		3.71 FeI
74.80	Cr	.104	.055	.053	.038		
81.97	CH	.009	.013	.007:	-		4.78 CH
82.41	Fe	.048	.040	.035	.043		4.43 FeI
83.01	Ca	.065	.015	.037	.022		4.48 CaI
87.90	Ni, Fe, TiII	.035	.019	.009	.024		4.73 TiII
89.36	Ca	.068	.020	.025	.041:		4.50 CaI
89.72	Cr	.083	.041	.047	.020		4.14 CrI
90.22	TiII	.063	.035	.030	.104		4.64 TiI
91.47	Fe	.020	.009	.011	-		4.69 FeI
93.12	CH	-	.031	-	-		4.71 CH
95.18	CH	-	.039	-	-		4.67 CH
96.74	FeII, CeII	.038	.020	.021	.041:		4.78 FeII ?
97.14	CH bl	.039	.022	.028	-		4.72 CH
98.99	Ca	.057	.026	.032	.035		4.49 CaI
4300.05	TiII	.120	.063	.073	.133		4.46 TiII
00.96	CH bl	.054	-	.045			

TABLE 3 (Continued)

λ	Ident.	HD 219617	HD 140283	HD 19445	HD 161817	Back-ground HD161817	Identifications -log W/λ ⊙
4301.93	TiII	.078	.031	.033	.060		4.60 TiII
03.13	FeII	.050	.022	.022	.043		4.72 FeII
03.94	CH	.059	-	.036	-		4.66 CH
07.87	CH,Fe,TiII	.288	.156	.183	.122		3.72 FeI
11.57	CH bl	.042	-	.022	-		4.78 CH, FeI
12.21	CH bl	.043	-	.022	-		4.84 CH
23.23	CH	.041	-	.021	-		4.71 CH, FeI
23.98	CH bl	.038	-	.024	-		4.74 CH
25.78	Fe	-	.095	.120	.105		3.81 FeI
37.05	Fe	.055	.043	.033	-		4.37 FeI
75.93	Fe	.073	.055	.054	.015		4.39 FeI
83.55	Fe	.221	.112	.160	.012		3.55 FeI
4404.75	Fe	.160	.093	.108	.088		3.66 FeI
15.13	Fe	.123	.071	.082	.065		3.92 FeI
15.56	ScII	.030	.012	.013	.022		4.49 ScII
16.83	FeII	.021	.008	.007	.045		4.63 FeII
17.71	TiII	.058	.024	.030	.10:		4.54
25.44	Ca	.069	.028	.037	-		4.38 CaI
30.62	Fe	.039	.015	.020	-		4.44 FeI
33.23	Fe	.022	-	-	-		4.66 FeI
35.69	Ca	.051	.022	.026	-		4.38 CaI
42.34	Fe	.063	.024	.028	-		4.27 FeI
43.80	TiII	.088	.055	.053	.073		4.45 TiII
44.56	TiII	.022	-	.009	.018		4.84 TiII
47.72	Fe	.045	.019	.019	.018		4.36 FeI
50.49	TiII	.052	.020	.024	.064		4.62 TiII

TABLE 3 (Continued)

λ	Ident.	HD 219617	HD 140283	HD 19445	HD 161817	Back-ground HD161817	Identifications -log W/λ ⊙
4461.65	Fe	.071	.035	.043	-		4.47 FeI
66.55	Fe	.063	.026	.031	.065		4.41 FeI
68.49	TiII	.073	.056	.053	.134		4.44 TiII
70.49	Ni	.016	.019	-	-		4.66 NiI
70.86	TiII	.008	.013	-	.013		4.80 TiII
81.24	MgII	-	-	.023:	.209		4.95 MgII
89.19	FeII	-	.013	-	.035		4.84 FeII ?
89.75	Fe	-	.008	-	.008		4.67 FeI
90.78	Fe	-	-	-	.010		4.81 FeI
91.41	FeII	-	-	-	.041		4.75 FeII
94.57	Fe	-	.023	.039:	.044		4.35 FeI
4501.27	TiII	.074	.056	.064	.126		4.53 TiII
08.23	FeII	-	.027	.024	.071:		4.69 FeII
15.34	FeII	.024	.023	.016	.063		4.78 FeII ?
26.94	Ca	.010	-	-	-		4.67 CaI
28.62	Fe	.090	.039	.041	.039:		4.31 FeI
31.15	Fe	.063	.018	.018	-		4.55 FeI
33.24	Ti	.039	-	.030	-		4.64 TiI
33.97	TiII,Co	.083	.048	.053	.107		4.59 TiII, Co
34.78	Ti	.026	.016	.023	-		4.70 Ti
35.93	Ti bl	.035	-	.031	-		4.73 TiI
48.78	Ti	.016	.017	-	-		4.83 TiI
49.62	TiII,FeII	.138	.073	.086	.216		4.43 TiII
54.03	BaII	.092	.020	.049	.069		4.39 BaII
58.65	CrII	.020	.036	.017	.063		4.80 CrII
63.76	TiII	.095	.043	.049	.108		4.53 TiII

TABLE 3 (Continued)

λ	Ident.	HD 219617	HD 140283	HD 19445	HD 161817	Back-ground HD161817	Identifications -log W/λ ⊙
4571.10	Mg	.030:	.046:	.053	-		4.66 MgI
71.97	TiII	.072	.060	.060:	.125		4.44 TiII
76.33	FeII	-	.026	.037	-		4.83 FeII
78.56	Ca	-	.023:	.008	-		4.72 CaI
83.84	FeII	.060	.039	.027	.122		4.47 FeII
88.21	CrII	.007 ?	-	-	.075:		4.81 CrII
89.96	TiII	.036	.019	-	.033:		4.74 TiII
91.40	Cr	.014	-	-	.002		4.88 CrI
4602.95	Fe	.036	.032	.033	-		4.54 FeI
46.17	Cr	.039	-	-	-		4.69 CrI
4703.00	Mg	.160	.051	-	.056		4.08 MgI
36.78	Fe	.060	-	.034	-		4.39 FeI
4871.31	Fe	.066	-	-	-		4.26 FeI
78.23	Fe	.070	-	-	-		4.49 FeI
90.76	Fe	.068	-	-	-		4.26 FeI

In HD 161817, the H lines are very strong, and the intensities are measured with respect to the background of the H lines. The following very weak and poor lines were measured for special elements.

λ	Ident.	HD 219617	HD 140283	HD 19445	HD 161817	Back-ground HD161817	Identifications -log W/λ ⊙
4150.97	ZrII		.003	.007:			5.13 Ti, ZrII
77.54	YII		.020	.017 bl			4.70 YII (Fe bl?)
86.62	CeII		.010	-			4.85 CeII -
4263.61	LaII		.006	.015:			5.36 LaII
4374.95	YII		.008	-			4.69 Mn,Co,YII

while the abscissa is

$$\log \eta_0 = \log \frac{N_{r,\,s}}{k\,(P_e, T)}\; a_0\,. \tag{1}$$

Here $N_{r,\,s}$ is the number of atoms per gram of stellar material in the lower level of the transition involved. It is related to N_r, the number of atoms in the rth stage of ionization, by the Boltzmann formula,

$$\frac{N_{r,\,s}}{N_r} = \frac{g_{r,\,s}}{u_r\,(T)}\; 10^{-5040\chi_{r,\,s}/T}\,, \tag{2}$$

where $u_r(T)$ is the partition function and $\chi_{r,\,s}$ is the excitation potential of the lower level. The quantity a_0 is the fictitious absorption coefficient at the center of the line (see, e.g., Aller 1953, p. 252, for notation), and $k(P_e, T)$ is the coefficient of continuous absorption, calculated per gram of stellar material for the mean temperature and pressure of the stellar atmosphere. Explicitly,

$$\eta_0 = \frac{\pi e^2}{m c}\, N_r\, \frac{g_{r,\,s}\lambda f}{\sqrt{(\pi)}\; k\,(P_e, T)\; v}\; \frac{10^{-5040\chi_{r,\,s}/T}}{u_r\,(T)} \tag{3}$$

There are several methods to determine the quantity N_r. The best estimate of the temperature of the atmosphere is obtainable from the color of the star or its spectral energy distribution. The electron pressure may be determined from the level of ionization or from the Stark broadening of the hydrogen lines. In addition to theoretical transition probabilities, f-values exist, with calibrations on an absolute scale. These are generally insufficient to determine the ionization equilibrium with sufficient accuracy. Unfortunately, the metals present in two stages of ionization have too small a range of ionization potential to yield both T and P_e.

The actual procedure was based on the empirical f-values, or $\log \eta_0^{\odot}$, obtained from the sun. For a group of unblended lines of atoms and ions we take the measured solar $\log W/\lambda$, and from the known solar curve of growth find $\eta_0^{\odot}$. We construct a stellar curve of growth and find η_0^{*}. The direct use of equation (3) give η_0/N_r, which involves the unknown f-values. The solar $\eta_0^{\odot}$'s, however, permit the elimination of f and provide the ratio $N_r^{\odot}/N_r^{*}$. The empirical η's have certain advantages when stars are compared that have temperatures not greatly different from that of the sun. Errors caused by stratification, fluorescence, or deviations from local thermodynamic equilibrium should enter the solar and stellar quantities in nearly the same way. Conditions in the sun are much better known than in the stars, and relative abundances of spectroscopically similar elements, with respect to the sun, may easily be modified with improved knowledge of the solar model.

Since most quantities will be measured by the mean logarithm of the ratio of their value in the sun to the corresponding value in the star, we shall introduce the notation

$$\left\langle \log \frac{X^{\odot}}{X^{*}} \right\rangle = [X]\,. \tag{4}$$

The curve of growth for the sun is the source of $\log \eta_0^{\odot}$. The mean value of the $\log \eta_0^{*}$ is obtained by superposition of $\log W/\lambda\ (c/v)$ in the star, for all lines of a given element, on the theoretical curve that best fits the lines of the reliably determined elements. The usual equation is, for each line.

$$\log \frac{\eta_0^{\odot}}{\eta_0^{*}} = \log \frac{N_r^{\odot}}{N_r^{*}} + \log \frac{k\,(P_e^{*}, T^{*})}{k\,(P_e^{\odot}, T^{\odot})} - \chi_{r,\,s}\,(\theta^{\odot} - \theta^{*}) + \log \frac{v^{*} u\,(\theta^{*})}{v^{\odot} u\,(\theta^{\odot})}\,. \tag{5a}$$

We rewrite it, for the mean of lines of the given element, in the stage of ionization, r, as follows:

$$[\eta] = [N_r] - [k] - \langle \chi_{r,\,s}(\theta^{\odot} - \theta^{*}) \rangle - [vu(\theta)]\,. \tag{5b}$$

From the shift required to fit all lines r, s of a given element, we obtain the mean value, $[\eta]$.

The weakness of the lines in these metal-poor stars makes the determination of the excitation temperature very uncertain. The data of Figure 1 indicate that the excitation temperature of HD 140283 is no higher, and actually may be lower, than that of the sun. Using the observed equivalent widths and the curves of growth for the sun and star, respectively, we obtain $[\eta]_{r,\,s}$ for each neutral iron line. When the results are plotted against the excitation temperature, the differences fall in a scatter diagram in such a way that it would be unwise to determine differences of excitation temperature. There is little doubt that, if anything, $[\eta]$ increases with increasing excitation potential. The diagram shows the results of a change of adopted $\Delta\theta$ amounting to 0.1.

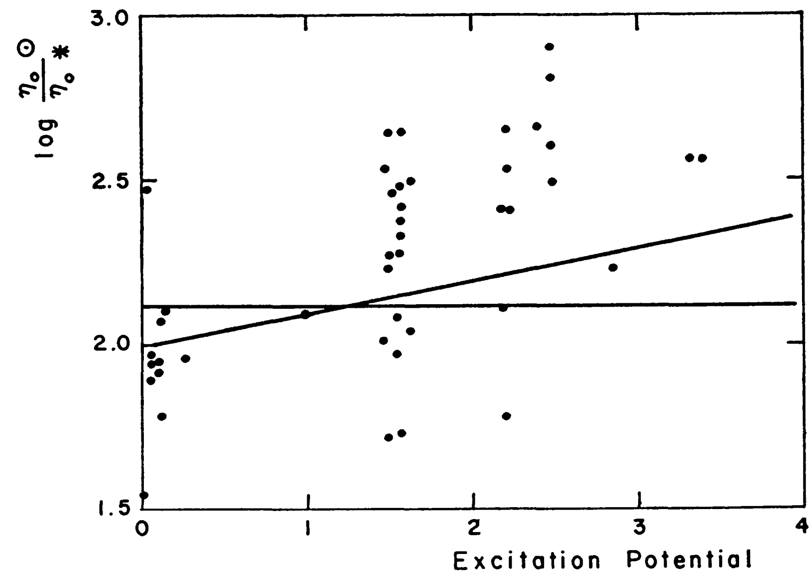

FIG. 1.—The excitation temperature for HD 140283 is poorly determined. The ratio of log $\eta_0^{\odot}/\eta_0^{*}$ for Fe I as a function of excitation potential is plotted on the assumption that $\theta_{\text{exc}}^{\odot} = \theta_{\text{exc}}^{*}$ (*horizontal line*). If any trend exists, it is in the sense that $\theta_{\text{exc}}^{*} > \theta_{\text{exc}}^{\odot}$; the line inclined upward is $\theta_{\text{exc}}^{*} = \theta_{\text{exc}}^{\odot} + 0.1$.

In the present analysis, therefore, we neglect the differences in the partition functions between these stars and the sun; likewise, we set the excitation temperatures for the sun and subdwarfs as equal. We still have the problem of choosing the ionization temperature and shall see that the composition depends very strongly on the temperature chosen.

Table 4 gives data on the colors, nominal spectral classes based on low-dispersion estimates, and temperatures of these high-velocity stars. We shall see that all except HD 161817 are G stars. The colors and spectral classes are from Nancy Roman (1955), except for a new color of HD 140283 by G. Abell. The temperatures for all but HD 161817 are based on the work of Melbourne (1959); they correspond to the effective temperatures of model atmospheres that reproduce the energy distribution measured by photoelectric spectral scans (resolution 10–20 A) after correction for blanketing by the metallic lines. The colors of subdwarfs are more nearly those predicted by such models than are the colors of normal stars, because of the large blanketing in the strong-lined stars. The effects are severe in the $U - B$ colors and still very substantial on the $B - V$ colors. Schwarzschild, Howard, and Searle (1955) determined the differences in blanketing between the sun and the G0 subdwarf HD 64090; the lines in HD 19445 are even weaker, and the blanketing is only one-fifth that in the sun. Melbourne finds that the continuous energy distribution in HD 19445 corresponds closely to that predicted for a model with the effective temperature, 5800° K, near that of the sun. Similarly, a model with the effective temperature of only 5450° K represents HD 140283 very well. Since HD 219617 was not measured with the scanner and has stronger lines, the blanketing values given by Schwarzschild *et al.* (1955) were used as corrections to the $B-V$, $U-B$ colors and give a somewhat uncertain value of $T =$ 5900° K. Note that the logarithms of abundance deficiencies derived from neutral lines will vary about as $6\,\Delta\theta$, where $\Delta\theta$ is the error in temperature. It seems unlikely that $\Delta\theta$ exceeds 0.04, unless there exists an unknown, non-gray source of opacity or a very peculiar temperature distribution in these stars. The calculation of the ionization equilibrium indicates that a temperature slightly lower than the effective temperature should be employed.

TABLE 4

COLORS, "NOMINAL SPECTRAL CLASSES": ADOPTED EFFECTIVE TEMPERATURES OF HIGH-VELOCITY STARS

Star HD	$B-V$	$U-B$	Temp. (° K)	"Nominal Spectral Class"
19445	$+0^{m}46$	$-0^{m}24$	5800	sdF7
140283	+ .48	− .14	5450	sdF5
161817	+ .16	+ .10	{7500: 8000	dA2
219617	+0.47	−0.20	5900:	sdF8

Then an additional uncertainty of about 0.02 in $\Delta\theta$ is introduced; total errors in logarithms of the abundances arising from the temperature are therefore less than 0.4. We have used ionization temperatures of 5700°, 5350°, and 5660° K for HD 19445, HD 140283, and HD 219617, respectively.

Table 5 gives the empirical values of log $\eta_0^{\odot}/\eta_0^{*}$, based on the observed equivalent widths and curves of growth. Entries indicated with a colon are considered to be very uncertain.

To obtain the abundances, we must know the level of ionization. Since all stars except HD 161817 have temperatures near that of the sun, we may neglect the variation in excitation temperature and partition functions. For a neutral atom,

$$[\eta]_0 = [N]_0 - [kv]\,, \tag{6a}$$

and, for an ion,

$$[\eta]_1 = [N]_1 - [kv]\,, \tag{6b}$$

where $[N]_0$ and $[N]_1$ are the logarithms of the relative concentration of neutral and ionized atoms of a given element in the sun as compared with the star. The ionization equilibrium is determined from

$$[\eta]_1 - [\eta]_0 = [N]_1 - [N]_0 \equiv \Delta\,. \tag{7}$$

We assume that neutral and ionized lines are produced in the same layer and fall in the same spectral region. The effects of the continuous absorption coefficient and of the velocities, which are presumably mostly thermal in the subdwarfs and both thermal and turbulent in the sun, are eliminated. The quantity Δ may be obtained for each (neutral atom-ion) pair for each star (see Table 6).

In order to estimate the electron pressure in the subdwarfs, we must make some assumptions about the electron pressure and temperature in the sun. For the line-forming regions we have adopted

$$\log P_e^{\odot} = 1.30 , \qquad \theta^{\odot} = 0.89 ,$$

corresponding to $\tau = 0.35$ (λ 5500), in the model atmosphere (Pierce and Aller 1951) adopted for the quantitative analysis of the solar atmosphere (Goldberg, Müller, and Aller 1960). The electron pressure is lower than that often adopted, e.g., by Unsöld (1948) for his "coarse analysis" of the sun, but seems more appropriate for our present purposes. A substantial improvement can be obtained only by going to model-atmosphere calculations.

TABLE 5

OBSERVED VALUES OF LOG $\eta_0^{\odot}/\eta_0^*$

Atom or Ion	HD 19445	HD 219617	HD 140283	HD 161817
CH	+1.50:	+1.20	+1.70:	....
Mg I	+0.55	+0.52	+1.50	+1.00
Mg II	....	....	....	−2.37
Al I	+1.50:	+1.34	+2.45	+2.02
Si I	+1.2:	+0.34	+1.74	+1.93
Ca I	+1.24	+0.85	+1.66	+1.53
Ca II	....	....	+1.05	....
Sc II	+1.23	+1.29	+1.35	+1.2:
Ti I	+1.02	+0.98	+1.15	+2.10
Ti II	+0.90	+0.44	+0.83	+0.11
V II	+1.3:	....	+0.73	....
Cr I	+1.67	+1.28	+1.44	+2.80
Cr II	+0.87	....	+0.20	....
Mn I	+1.33	+1.00	+1.45	+2.91
Fe I	+1.54	+1.14	+1.48	+2.10
Fe II	+1.08	+0.75	+0.83	+0.18
Co I	+0.32:	−0.06:	+0.88:	+1.01:
Ni I*	−0.79:	−0.87:	+0.50:	−0.01:
Sr II	+1.19	+1.28	+0.92	+0.76
Y II	....	....	+1.48::	....
Zr II†	....	....	+1.14::	....
Ba II	+1.31	+0.55	+1.44	+0.97

* See text for the nickel abundance.

† One line each of La II and Ce II included in this mean. All blended.

Table 6 gives the values of log $N_1^{\odot}/N_0^{\odot}$ calculated for Ca, Ti, Cr, and Fe with the previously mentioned solar values for temperature and electron pressure. For each of the three subdwarf stars there are four columns, which give, successively, Δ, log N_1^*/N_0^* calculated from equation (7), log $(N_1^*/N_0^*)P_e$ computed from the ionization equation with the adopted θ, and, finally, the value of log P_e. The mean value of log P_e is obtained by assigning greater weights to iron and titanium than to the other elements. Notice that the electron pressures in HD 19445 and HD 219617 are equal to within the errors of the determination but that the electron pressure in the cooler star, HD 140283, is substantially lower. The last row of the table gives the ratio of the absorption coefficients calculated for λ 4000 from Allen's tables (1955) with the given values of θ and log P_e. Similar values are obtained for λ 4235 from unpublished tables by Strömgren.

At the low metal abundances of the subdwarfs, the source of electrons is the ionization of hydrogen rather than of the metals. The opacity is largely the negative hydrogen ion, and the usual tables which give k_λ (θ, P_e) are still valid. The range of spectral types in which the electrons still come dominantly from hydrogen is extended toward cooler stars. The relation between P_e and P_g is radically different. Since few lines are strong enough to show pressure broadening, the change in $[\eta]$ is by a factor of $[1/A]$ when the hydrogen-to-metal ratio, A, increases. At lower temperatures the $[\eta]$ for most lines is independent of $[A]$ and becomes proportional to $[A]$ for lines affected by pressure broadening. Our early G subdwarfs still can show line weakening, and P_e is P_g/A or greater.

The curves of growth for these stars are moderately well determined. We show the best of these, HD 140283, in Figure 2. A fit of the empirical log W/λ, log η plot to the theoretical curves shows no indication of turbulence. The most probable velocity, v, is that appropriate to a kinetic temperature of 5500° K. Similar results are obtained in the other subdwarfs.

TABLE 6

LEVEL OF IONIZATION AND PARAMETERS OF SUBDWARF ATMOSPHERE

Element	log $(N^{\odot}/N_{\odot})$	HD 19445, $\theta_{ion}=0.884$				HD 140283, $\theta_{ion}=0.94$				HD 219617, $\theta_{ion}=0.89$			
		Δ	log (N_1^*/N_0^*)	log $(N_1^*/N_0)P_e$	log P_e	Δ	log (N_1^*/N_0^*)	log $(N_1^*/N_0^*)P_e$	log P_e	Δ	log (N_1^*/N_0^*)	log $(N_1^*/N_0^*)P_e$	log P_e
Ca	2.62	.....	.....	.....	.....	0.61	3.23	3.56	+0.33	.....	.....	.....	.....
Ti	2.04	0.12	2.16	3.38	1.22	0.32	2.36	2.93	+ .57	0.54	2.58	3.34	0.76
Cr	1.72	.80	2.52	3.07	0.55	1.24	2.96	2.61	− .35	.....	.....	.....	.....
Fe	1.00	0.46	1.46	2.36	0.90	0.65	1.65	1.84	+0.19	0.39	1.39	2.30	0.91
Mean log P_e	.....	.....	.....	.....	0.90	.....	.....	.....	+0.34	.....	.....	.....	0.85
log $k_\lambda^{\odot}/k_\lambda^*$	.....	.....	.....	.....	0.40	.....	.....	.....	+0.82	.....	.....	.....	0.42

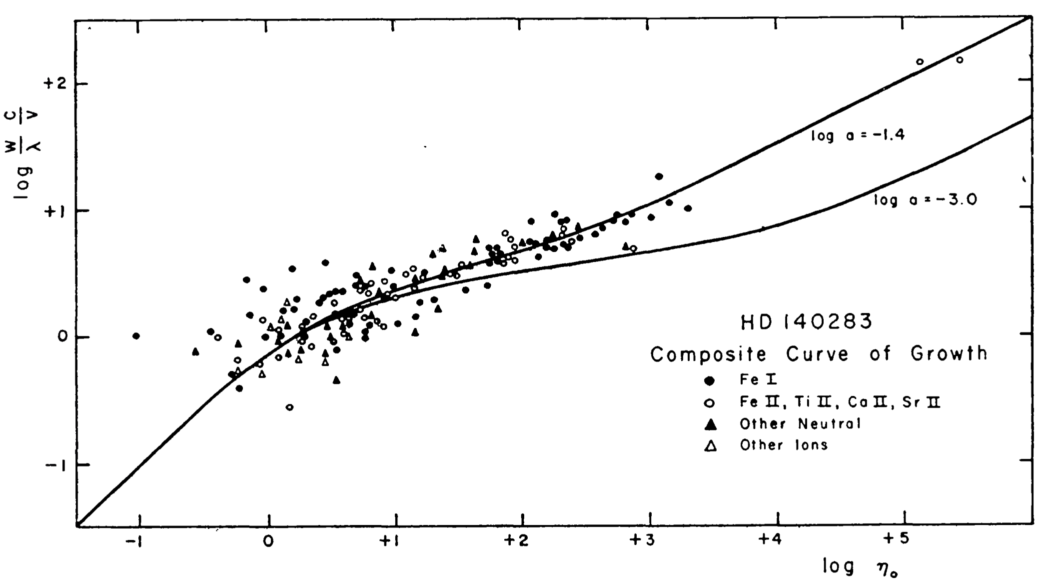

FIG. 2.—The curve of growth for HD 140283, the most accurately determined of the group of stars. The theoretical curve is for zero turbulence. The neutral atoms and ions are shown with different symbols. The damping constant is apparently high.

Table 7 illustrates in detail the analysis as carried out for HD 140283. From equation (5*b*) we may write the relative abundance thus:

$$[N] = \log \frac{N^{\odot}}{N_r^{\odot}} - \log \frac{N^*}{N_r^*} + [\eta] + [v] + [k] \, . \tag{8}$$

The excitation temperature and partition function terms disappear. The first two terms on the right are the levels of ionization in sun and star, determined by data of Table 6. These ionization corrections are listed in the first and second columns of Table 7.

TABLE 7

CALCULATION OF ABUNDANCES OF ELEMENTS

Element	Solar $N^{\odot}/N_r^{\odot}$	Abundances: HD 140283				
		Stellar (N_r^*/N^*)	$\log (v^{\odot}/v^*)$	$\log (N^{\odot}/N^*)$	HD 19445 $\log (N^{\odot}/N^*)$	HD 219617 $\log (N^{\odot}/N^*)$
C*	....	....	....	3.40:*	2.25:*	1.95:*
Mg I	23.4	0.0136	0.07	1.87	0.58	0.58
Al I	64.1	0.0040	.08	2.73:	1.54:	1.40:
Si I	3.8	0.103	.09	2.23	1.2:	0.49
Ca I	418	0.00059	.18	2.02	1.37	1.01
Ca II	1.01	1.00	....	2.03	....	....
Sc II	1.005	1.00	.21	2.34	1.84	1.92:
Ti I	111	0.0025	.22	1.72	1.20	1.17
Ti II	1.01	1.00	....	1.85	1.52	1.08
V II	1.015	1.00	.23	1.76	1.93:	....
Cr I	53.5	0.00537	.24	1.94	1.86	1.50
Cr II	1.02	1.00	....	1.25	1.51	....
Mn I	25	0.0122	.25	1.99	1.54	1.22
Fe I	11.0	0.0306	.25	2.06	1.75	1.39
Fe II	1.10	0.97	....	1.91	1.75	1.44
Co I	8.4	0.039	.25	1.45:	0.55:	0.23:
Ni I*	6.1	0.0555	.26	1.42*	1.53*	1.38*
Sr II	1.00	1.00	.35	2.03	1.92	2.04
Y II	1.00	1.00	.35	2.59::	....	....
Zr II†	1.00	1.00	.36	2.30::	....	....
Ba II	1.015	0.782	0.45	2.59	2.15	1.40

* See text for analysis of C abundance and for Ni.

† One line each of Zr II, La II, and Ce II is included in this poorly determined mean. The lines of these heavy elements are all weak and blended.

There is a mass-dependent variation in [*v*], since the sun has turbulence and the star only thermal motions; this correction is given in the fourth column. The value of [*k*] is obtained from the opacity tables, using θ and P_e from Table 6. The abundance ratio, sun to star, is in the last column. The value for C is obtained from CH and is discussed below. The accordance between abundances based on [η] for neutral and ionized elements is satisfactory. The final results, in abbreviated form, are given for HD 19445 and HD 219617 in the last two columns of Table 7.

The second ionizations can be neglected for nearly all atoms. The results are uncertain for the heavy elements and for Co I which are represented by only a few lines. The abundance deficiencies in these three stars are very large and, in spite of large experimental errors for many elements, have essentially the same pattern. Abundance deficiencies of the order of 30–50 for most of the metals, smallest in HD 219617 and reaching a factor of 100 in HD 140283, are well established. There is also a clearly established difference between HD 219617 and HD 140283, so that not all population II "subdwarfs" are identical.

The only possible explanation, other than real abundance differences, is that an unknown source of opacity exists in these population II stars. It should exceed H^- by a large factor if the composition were the same as in the sun. It is difficult to see how such a new source could exist in a star in which the abundances of all elements but hydrogen are apparently low. No evidence on helium exists, but we cannot suggest any unstable radical or compound for it. If C, N, or O were very overabundant, possibly their negative ions might become important. We shall see that C has almost certainly an even lower

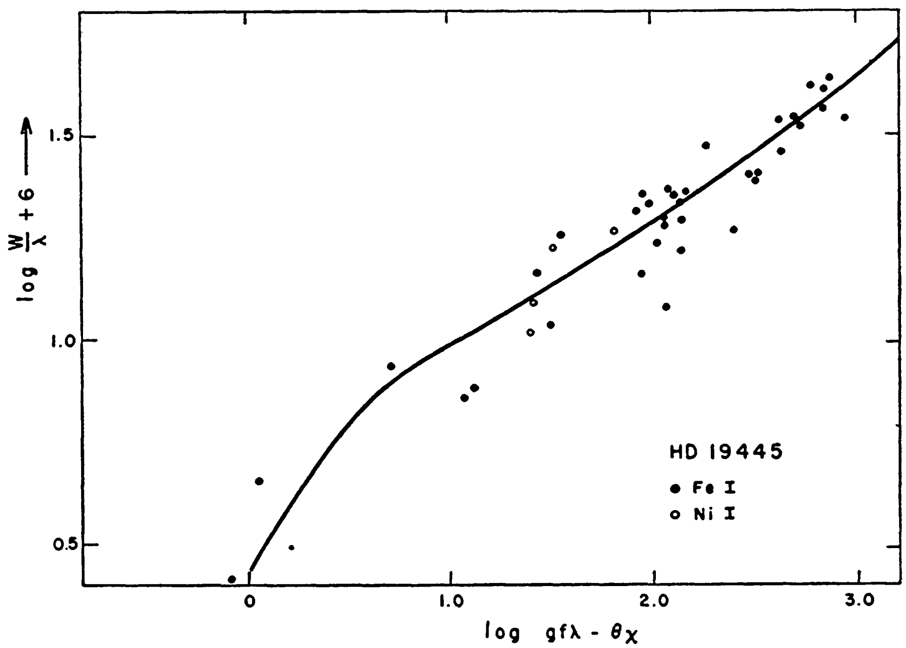

FIG. 3.—The curve of growth of iron and nickel in HD 19445. Since the Ni lines are largely in the ultraviolet, solar η_0's are unsatisfactory. Laboratory gf-values from King are used, adjusted to an absolute scale.

relative abundance than the metals. No bands of CN are seen in G subdwarfs. In a poor infrared exposure of HD 140283 the lines of O I were absent; the lines of C I and N I, weak in normal stars, are not present in the photographic region of the subdwarf spectra.

The problem of nickel deserves special mention. Most of the lines fall in the ultraviolet region below λ 3900, where the solar spectrum is strongly affected by the blending of strong lines, whereas the subdwarf is not. The empirical log $\eta_0^{\odot}$'s will be systematically decreased, since the log $W^{\odot}$'s from which they are derived are too small. Accordingly, we have calculated the abundance of nickel by making plots of log W/λ versus log $gf\lambda-\theta\chi_{r,s}$ for both nickel and iron and fitting these plots to the theoretical curve of growth. There we use the laboratory gf-values (King 1938, 1948) for both iron and nickel, with scaling factors to reduce relative to absolute gf-values from the solar abundance studies of Goldberg, Müller, and Aller (1960). The Ni/Fe ratio in the sun and subdwarfs will be affected by exactly the same amount through an error in the calibration of the nickel f-values. Figure 3 shows the empirical curve of growth for HD 19445 obtained in this manner. Since we have laboratory gf-values for Fe I, we may use the Fe I lines from all regions of the spectrum; the Ni I lines in the ultraviolet are located on a continuum which is hardly depressed. The calibration of the Ni and Fe gf-values by Goldberg, Müller, and Aller is not affected by the depressed ultraviolet of the sun, since it is based on a wide range of wave lengths. The data for HD 161817 are discussed below. The weakest-line star, HD 140283, has an Fe/Ni ratio about four times as high as the sun. (see Table 8). Our preliminary analysis, using solar values for Fe I and Ni I actually gave the Ni abundance greater than that of Fe. We could have expected such a conclusion from the log $\eta_0^{\odot}/\eta_0^{*}$ of Table 5, in which the deviation from the solar values is -0.8 for Ni and $+1.5$ for Fe. The special analysis seems reliable, and the relatively high abundance of Ni is significant in theories of nucleogenesis. An apparently high ratio of Co/Fe is also found in the subdwarfs, but the experimental data are very poor.

TABLE 8

RELATIVE ABUNDANCES OF IRON AND NICKEL

Star	log N(Fe)/N(Ni)	Star	log N(Fe)/N(Ni)
Sun................	+1.08	HD 161817........	+1.19
HD 19445..........	+0.86	HD 219617........	+1.04
HD 140283.........	+0.52		

THE CH MOLECULE

In addition to the lines of the metals, the lines of the molecule CH also appear in a number of the subdwarfs. From a comparison of their equivalent widths in the sun and in subdwarfs, we can estimate indirectly the abundance of carbon in these stars.

The equilibrium constant for the dissociation of the CH molecule is related to the partial pressures of C, CH, and H by

$$K_{\mathrm{CH}}=\frac{p_{\mathrm{C}}p_{\mathrm{H}}}{p_{\mathrm{CH}}}=\frac{N_{\mathrm{C}}}{N_{\mathrm{CH}}}P_g\,. \tag{9}$$

The pressure of hydrogen is essentially the total gas pressure. Then

$$[N_{\mathrm{CH}}] = [N_{\mathrm{C}}] + [P_g] - [K_{\mathrm{CH}}]\,. \tag{10}$$

In the atmospheres of both the sun and the subdwarfs, the molecules tend to be concentrated in the uppermost layers. The molecular lines probably cannot be compared as meaningfully by means of the curve of growth at the same temperature and atmospheric depths as can the other lines in the spectrum.

We shall have to make use of model atmospheres, although in a somewhat schematic way. The temperature distribution is assumed to be given by

$$T^4=\tfrac{3}{4}T_{\mathrm{eff}}^4\left[\tau+q(\tau)\right], \tag{11}$$

where $q(\tau = 0)$ is evaluated by the theory proposed by Chandrasekhar (1936) for the blanketing effect. Let $\bar{k}$ denote the mean absorption coefficient, including both the lines and the continuum. Let β denote the fraction of the outgoing radiation stopped by absorption lines whose absorption coefficient is $k_2 = x_1\bar{k}$, while the absorption in the continuum is $k_c = x_2\bar{k}$. Then

$$q(0)=\frac{1}{\sqrt{\{3\left[\beta x+(1-\beta)\,x_2\right]\}}}\,. \tag{12}$$

For the sun, $\beta = 0.124$ (Michard 1950), and we choose $x_1 = 20$ and $x_2 = 0.85$. For the subdwarfs, we estimate $\beta = 0.023$, while $x_2 = 0.95$. Hence we obtain a boundary temperature T_0 of 4500° K for HD 19445, 4250° K for HD 140283, and 4000° K for the sun.

Let us assume, for the time being, that the molecular lines are formed in layers with essentially the boundary temperature, T_0. Then, using the results by Pecker and Peuchot (1954) for $K_{\mathrm{CH}}(T)$, $\log K_{\mathrm{CH}}(\odot)/K_{\mathrm{CH}}(*) = -0.30$ (HD 140283) and -0.54 (HD 19445, HD 219617). We have next to evaluate the electron pressures and gas pressures for these outer layers in the subdwarfs and in the sun. In the sun the metals supply the electrons; in the subdwarfs the electrons are supplied by hydrogen in the layers where the normal metal lines are formed, but predominantly by the metals in the cooler layers, $T < 4500°$ K. Hence, in these outer layers, $P_e/P_g \approx 1/A$, where A is the ratio of hydrogen to the metals—even for metal depletions amounting to as much as log $A = 5.8$. Then, just as in equation (5), we have

$$[N_{\mathrm{CH}}] = [\eta_{\mathrm{CH}}] + [v] + [k] . \tag{13}$$

Neglecting the difference between the thermal velocities in the sun and the subdwarf, we obtain, from equations (9), (10), and (13),

$$[N_{\mathrm{C}}] = [\eta] + [k_0] + \frac{P_e}{P_g} + [K_{\mathrm{CH}}] , \tag{14}$$

since $k(P_e, T) = k_0(T)P_e$ for the negative hydrogen ion. In this region, $P_e/P_g \approx 1/A$, and we find

$$[N_{\mathrm{C}}] = [\eta] + [k_0] - [A] + [K_{\mathrm{CH}}] . \tag{15}$$

The abundances of carbon are

$$[N_{\mathrm{C}}] = [\eta] + 0.09 - [A] - [0.54] , \quad \text{for } T_0 = 4500° \text{ K} ,$$

$$[N_{\mathrm{C}}] = [\eta] + 0.05 - [A] - [0.30] , \quad \text{for } T_0 = 4250° \text{ K} .$$

Since $[A]$ is about -2.0 for HD 140283 and -1.5 for the other stars, the results are

$$\log \frac{N_{\mathrm{C}}^{\odot}}{N_{\mathrm{C}}^{*}} = \log \frac{\eta^{\odot}}{\eta^{*}} + 1.05 = 2.55 , \qquad \text{HD } 19445$$

$$= 2.25 , \qquad \text{HD } 219617 ,$$

$$\log \frac{N_{\mathrm{C}}^{\odot}}{N_{\mathrm{C}}^{*}} = \log \frac{\eta^{\odot}}{\eta^{*}} + 1.70 = 3.40 , \qquad \text{HD } 140283 .$$

We next examine the consequences of the assumption that the molecular lines are formed in the same layers as the metallic lines. We use equation (14) but cannot assume $P_e/P_g \approx 1/A$ in these layers. We find the value of P_e/P_g for an optical depth of 0.4. No model atmosphere has been computed for log A values as high as 5.3–5.8; Swihart (1956) gives models with solar temperature for log $A = 3.8$ and 5.0, i.e., with a difference of A equivalent to $[A] = 1.2$. An examination of his Table 1 shows that $[P_g/P_e] = -0.59$, very nearly $[A^{1/2}]$. With these crude data we extrapolate and obtain

$$[N_{\mathrm{C}}] = [\eta] + [k_0(\tau = 0.4)] - [A^{1/2}] + [K_{\mathrm{CH}}] . \tag{16}$$

Then the abundances of carbon are

$$\log \frac{N_{\mathrm{C}}^{\odot}}{N_{\mathrm{C}}^{*}} = [\eta] + 0.75 = +2.25 , \qquad \text{HD } 19445$$

$$= +1.95 , \qquad \text{HD } 219617 ,$$

$$\log \frac{N_{\mathrm{C}}^{\odot}}{N_{\mathrm{C}}^{*}} = [\eta] + 1.20 = +2.90 , \qquad \text{HD } 140283 .$$

The observational errors correspond to a factor of 2 in HD 140283; the theoretical analysis may introduce even larger errors.

Within the uncertainties involved, the deficiency of carbon is as large as, or larger than, that of the metals! A final solution will depend on details of model-atmosphere analysis. The steep dependence of the dissociation constant, K_{CH}, on temperature favors the first hypothesis of molecular lines at small τ, which gave an abundance deficiency of C by almost 1000.

The CH lines are extraordinarily weak in these stars, and we have used individual lines and a blend of two CH lines. While the observational error is about ± 0.3 in $[\eta]$, we find that the CH lines are relatively weaker than the metallic lines. In later subdwarfs the G band appears more strongly. There are no definite indications of CN. A few weak lines in Table 2, for HD 19445, are listed as CN⊙, meaning that they are identified as CN in the sun. There is no proof that they are CN in this star. Table 2 gives some individual lines near the λ 4215 head as blends of CN in the sun; our measured equivalent widths are about 6 mA in HD 19445.

THE A STAR, HD 161817

HD 161817 suggests several puzzling questions. Its luminosity, while unknown, is probably near +1 to +2.5, occupying an unusual position in the HR diagram in population II. Its space motion is very large, its rotation very small. It shows λ 4481 of Mg II, which is rarely or never visible in the faint blue stars of the halo population. The Burbidges (1956) assigned an effective temperature of 8400° K, an ionization temperature 10 per cent lower, and log P_e = 1.80. Under such assumptions, there are only small metal deficiencies. Our material for this star is less extensive than for the others. The effective temperature can be estimated to be somewhat lower than 8400° K from the color, but no spectral scans or model-atmosphere computations are available. Consequently, we analyze our observations on two assumptions, (1) T_{ion} = 7500° K, log P_e = 1.40; (2) T_{ion} = 8000° K, log P_e = 1.85, which are both compatible with the level of ionization of Fe and Ti. The discussion by Bonsack *et al.* (1957) of the $B-V$, $U-B$, color-temperature scale suggests that the lower temperature might be preferable.

TABLE 9

DERIVED ABUNDANCES IN HD 161817

Element	log $N^{\odot}/N^*$		Element	log $N^{\odot}/N^*$	
	T=7500°	T=8000°		T=7500°	T=8000°
Mg I	−0.66	−1.16	Cr I	+1.40	+0.96
Al I	+0.75	+0.37	Mn I	+1.40	+0.90
Si I	+0.38	−0.13	Fe I	+0.51	−0.04
Ca I	+0.34	−0.09	Fe II	+0.68	+0.17
Sc II	+1.66	+1.14	Co I	−0.57	−1.05
Ti I	+0.69	+0.25	Sr II	+0.85	+0.29
Ti II	+0.54	+0.04	Ba II	+0.80	+0.24

Table 9 gives the results based on $[\eta]$ from Table 5. The preferred lower temperature suggests a mean underabundance factor of about 3 or 4; at the higher temperature, although the abundances are badly scattered, their average is nearly unity. A small abundance deficiency may be established if the color-temperature data are improved.

The analysis of Ni I lines must be done in the same way as in the G subdwarfs. We fitted plots of log W/λ against log $gf\lambda - \theta\chi$ for both Fe I and Ni I and, from the horizontal shift, determined log N(Ni)/N(Fe) = +1.19, very close to the value in the sun (see

Table 8). (We rejected the λ 3783 line of Ni I, which seems abnormally strong in HD 161817). The Mg abundance, which may be derived from the λ 4481 line, depends very critically on the assumed excitation temperature. The data from Mg I suggest an unexpectedly high abundance of Mg.

GENERAL CHARACTERISTICS OF SUBDWARF SPECTRA

No detailed spectroscopic classification scheme is as yet available for the very weak-lined stars. It is known that line weakening is very great in the so-called F subdwarfs, which from our analysis seem in fact to be G stars. The line weakening is much smaller in such so-called G subdwarfs as Groombridge 1830 (which from an unpublished analysis by Greenstein seems to be an early K star). Greenstein finds, from investigation of 18-A/mm spectra, that, when high-velocity subdwarfs are grouped by apparent excitation temperature, the hotter stars show a wide variety of line weakening and only a few of the cooler ones show detectable line weakenings. The theory giving the P_e/P_g ratio as a function of A and θ predicts this effect.

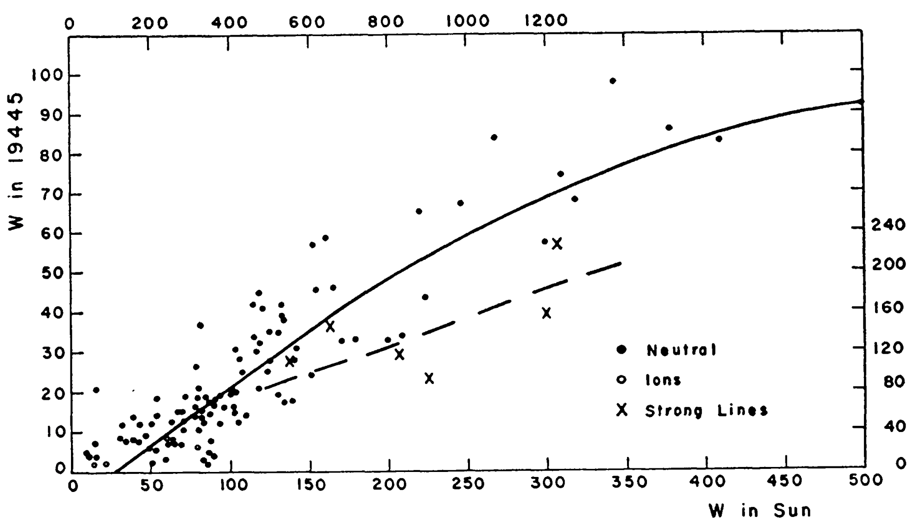

FIG. 4.—The measured equivalent widths, W, in milliangstroms for lines in HD 19445, as compared with W in the sun. The ions are slightly stronger relatively. The scale of W, at the top and right side of the figure, refers to the stronger lines. The dashed line is the mean relation for the strongest lines, the solid line for the weaker.

Since all our stars except HD 161817 have temperatures near the sun, a comparison with the sun and with each other is of some interest. Figures 4, 5, and 6 show the results in graphical form. We plot the equivalent widths in one star against those in another, indicating by special symbols the ions and a few elements of special interest. The differences in intensities and curves of growth result in a considerable variety in these relationships. Figure 4 compares HD 19445 and the sun. The lines in the sun are about five times as strong; even the very strong lines show about the same ratio. The lines of ionized elements are relatively stronger in the subdwarf, confirming our result that HD 19445 is slightly hotter. Figure 5 compares HD 19445 and HD 140283 and shows that the strength of weak lines is quite similar in both stars and that the ions are weaker in HD 140283, consistent with its lower temperature. A few strong lines are weaker, notably Mg, Al, and Ca, reflecting both a different curve of growth and a possible small abundance difference. Figure 6 shows that two subdwarfs of nearly equal temperature can have different line intensities and consequently different general deficiencies. HD 219617, which Greenstein (1956) has called an "intermediate subdwarf," has lines which are, on the average, 50 per cent stronger than those in HD 19445, although still much weaker than the sun. There is apparently no difference in the ratio of neutral and ionized lines between the two stars. A similar comparison, not reproduced here, of only the ultraviolet lines of Fe and Ni shows that in HD 140283 the Ni lines definitely fall above

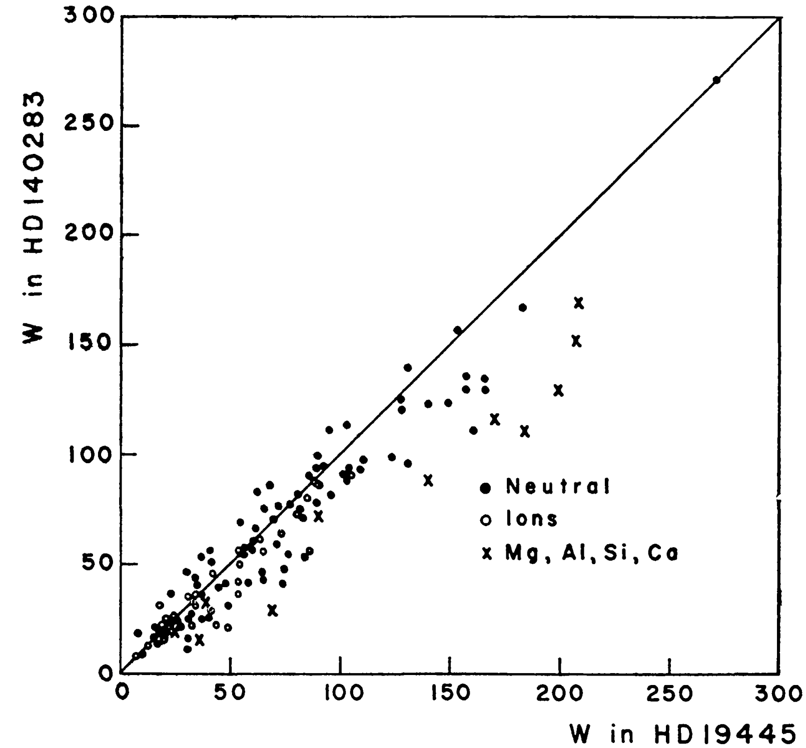

FIG. 5.—Comparison of W in HD 140283 and HD 19445. The solid line is at 45°. Some strong lines and especially Mg, Al, Si, and Ca fall abnormally low in HD 140283. Ions are also slightly weaker in HD 140283 relative to the average neutral atom.

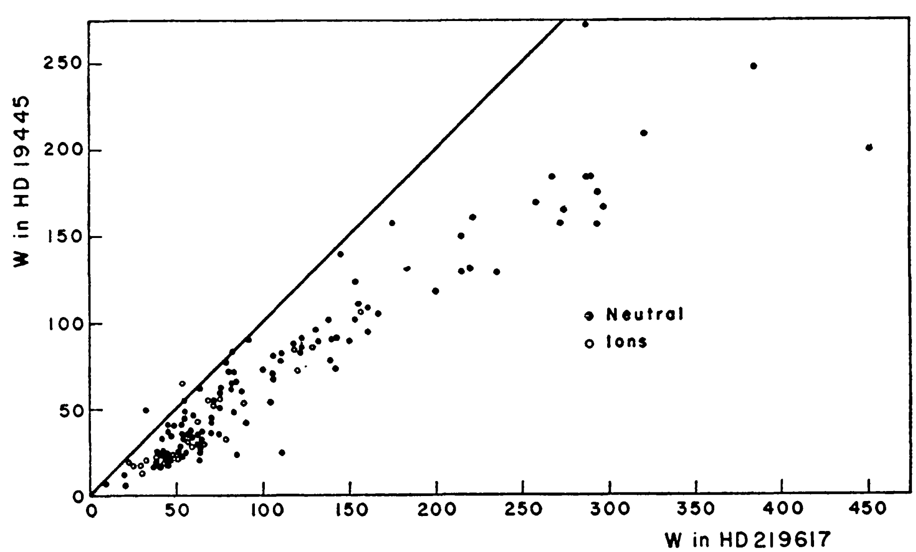

FIG. 6.—Comparison of W in HD 19445 and in the "intermediate" HD 219617. Note that nearly all lines fall below the 45° line. The behavior of lines of the ions and of neutral atoms is very similar.

the mean relation between equivalent widths in HD 140283 and in the sun. We believe that our analysis strongly suggests a larger ratio of Ni to Fe in HD 140283 than in the sun. Thus the visual appearance of subdwarf spectra gives many of the essential features of the complete analysis. Very careful estimates of line intensities may yield new information on other details of abundance changes between subdwarfs and normal stars.

PROBLEMS IN NUCLEOGENESIS

The accuracy of the determination of abundances of individual elements in subdwarfs is still low, even when these are with respect to the sun. The value of log A in the sun has been adopted as +3.8 in our brief consideration of models. The relative abundances of the average metals, sun/star, given in Table 7 can provide a new value of log A in the subdwarfs. We have weighted the individual values of $[N]$ in accordance with our estimate of reliability, with results given here. Weighted mean abundance of the metals: 3.80 for sun adopted; 5.39 for HD 19445; 5.78 for HD 140283; 5.07 for HD 219617. The extreme subdwarfs have metal deficiencies of the order of 40 and 100, and the intermediate, 20.

TABLE 10

MEAN WEIGHTED ABUNDANCE RATIOS, SUN/STAR, FOR AN EXTREME SUBDWARF

Element	$\langle [N] \rangle$	$\langle [N] \rangle = \log N^{\odot}/N^*$			Group Deviation from Mean	Group No. of Lines
		Main Nucleogenetic Processes	No. of Lines	Group Mean		
C	2.77	He-burning	7	2.77 (He)	+1.02	7
Mg	1.23	α	7	1.51 (α)	−0.24	17
Al	2.12	s	2	2.13 (s)	+0.38	12
Si	1.60	α	1	...	...	...
Ca	1.69	α	9	...	...	...
Sc	2.11	s	2	...	...	...
Ti	1.53	e	24	...	...	...
V	1.83	e	1	...	...	...
Cr	1.62	e	5	...	...	...
Mn	1.71	e	3	...	...	...
Fe	1.81	e	90	1.70 (e)	−0.05	123
Co	1.10	e′	1	...	...	...
Ni	1.45	e′	5	1.27 (e′)	−0.48	6
Sr	2.00	s	2	...	...	...
Y*	2.36::	s	2	...	...	...
Zr†	2.07::	s	3	...	...	...
Ba	2.24	s	1	...	...	...
Weighted mean	1.75	...	...	...	...	...

* HD 140283 only; group mean readjusted for fact that only one, extreme-low-abundance subdwarf used. Lines blended.

† HD 140283 only, readjusted as above. In addition, since all lines of Zr II are blended, we have included one line each of Ce II and La II; i.e., Zr represents a very rough determination for heavy elements. The weight, as given by the number of lines is less than this number would indicate, since only one star was used.

Another possible mode of analysis is to group together the abundances of each element in these stars, weighting them roughly in proportion to their deviation from the sun and the quality of the observational material. The weights assigned were 2 for HD 19445; 3 for HD 140283; and 1 for HD 219617. In Table 10 we list the resulting values of $\langle [N] \rangle$ for such a hypothetical average subdwarf. It has mean properties intermediate between HD 19445 and HD 140283. The accidental errors of the individual abundances are considerably reduced. However, we must note that any errors of method, or especially errors in solar η_0's are common to all stars. With caution, we may note some interesting results. The mean value of log $A = +5.55$. There is considerable scatter from the average $\langle [N] \rangle$ of a systematic type. In Burbidge, Burbidge, Fowler, and Hoyle (1957), the final table in the appendix gives a suggested nucleogenetic process that dominates for each isotope. In our Table 10, we list the dominant process for each element, assuming that the stellar isotope ratios are the same as in the sun and limiting ourselves to the most abundant isotope. Elements belonging to such a natural group are distinguished by their mode of origin: (1) helium-burning reactions in hot cores of red giants, 10^8–2×10^{8}° K; (2) α, alpha-particle reactions involving exchanges of α particles among C^{12}, O^{16}, and Ne^{20} at about 10^9° K, forming heavier elements, like Mg^{24}, Si^{28}, Ca^{44}; (3) s, the slow neutron-capture chain, building certain nuclei on the Fe peak elements and on some lighter nuclei; (4) e, the equilibrium process, at very high T, about 3×10^9° K in supernovae, forming the Fe peak abundances; and (5) e′ (our distinction), elements at the heavy side of the Fe peak. When the elements are so grouped, we find the means given in the fifth column of Table 10, and their deviation from the over-all mean in the next column. Compared to the over-all mean, (1) the simple helium-burning nucleus, C^{12}, is very underabundant (if our analysis of CH is correct); (2) the light nuclei, in which both high-temperature processes contribute, may be slightly more abundant than average; (3) the slow-neutron nuclei, s-process, and especially the heavier magic-number nuclei may be less abundant; (4) the e-process agrees with the over-all mean, except that (5) e′, the heavier e-process nuclei, Co and Ni seem overabundant.

If the ascriptions of elements to various origins are correct, or rather *were* correct in the very early history of the Galaxy when the elements composing these subdwarfs were formed, we can draw some speculative general conclusions about the types of stars then forming heavy elements. Fewer stars made C^{12}. The lack of C^{12} and presumably, therefore, of C^{13}, O^{17}, and Ne^{21} meant that there were fewer sources of neutrons in red giants with a residual hydrogen-burning outer zone. The supernovae that produced e-process elements also produced more Ni, i.e., were probably hotter. The ratio of e-process to s-process nuclei is greater than in average star formed at a later time.

The most striking effect and one which will require more detailed study in other very old stars is the apparent discrepancy between the helium-burning and the alpha-process nuclei. C^{12} is very underabundant, and Mg, Si, and Ca are relatively more abundant. There are two possible explanations:

1. A large amount of C^{12} was formed which later went through a hydrogen-burning zone. In that case, N^{14} would become the main product of He-burning, and C^{12} would not be very abundant. Excessive N abundance has been suggested repeatedly in such objects as the hot subdwarfs. However, in F or G stars, lines of N I would be weak, and probably only CN could be used to obtain the N abundance. CN is very weak in these stars. A special search for CN in late G or early K subdwarfs and for the infrared N I lines in F subdwarfs is planned.

2. If all C^{12} formed at 2×10^8° K was subjected to very high temperatures in a helium-rich atmosphere, the equilibrium concentration would result in the formation of the alpha-particle nuclei like Mg^{24} and Si^{28} from C^{12}. If one examines the actual abundances of C, Mg, and Si, as deduced from the solar values and our abundance deficiencies, it is apparent that any formation of Mg and Si in early-generation stars would seriously deplete C.

The reality of these effects remains to be discussed. The abundance ratios of individual elements, star/sun, is at times based only on a few lines, which may also be blended differently in these stars and in the sun. The statistical combination of the three G subdwarfs should be relatively free of errors except those in the solar data. The low abundance of C, based on the CH bands, suffers mainly from the uncertainty of the constants used and the computations of dissociation equilibria. Our analysis of the results of changes in level of formation in a rough model atmosphere indicate that stratification has only small effects. The second analysis of the Ni/Fe ratio, based on laboratory f-values, shows that the difference exceeds its probable error. Elements like Ba and some other heavy, s-process nuclei, for which very few lines are available, occur only as ions. For these, a model-atmosphere analysis might lead to different results, and the accidental errors are large. Our impression, nevertheless, is that there are real differences in the relative abundances of some elements, notably C and Ni and possibly some s-process nuclei.

THE PROFILES OF THE HYDROGEN LINES

We have also measured the profiles of the hydrogen lines and the K line of Ca II. Table 11 contains reflected mean profiles of lines of the Balmer series and the K line.

TABLE 11

RESIDUAL INTENSITIES, IN PER CENT, OF MEAN REFLECTED AND SMOOTHED PROFILES

Stars: a = HD 19445, b = HD 140283, c = HD 161817, d = HD 219617. Δλ in Angstroms

Δλ	Hβ				Hγ				Hδ				Hε		K				H8				H9			
	a	b	c	d	a	b	c	d	a	b	c	d	c	d	a	b	c	d	a	b	c	d	a	b	c	d
20....	...	...	95	...	...	...	98	...	...	...	96	...	96	...	...	...	...	...	...	...	98	...	...	...	...	...
15....	...	...	90	...	...	...	92	...	...	...	92	...	91	...	...	...	...	...	...	...	92	...	...	...	...	...
10....	...	...	82	...	98	99	84	...	98	...	83	98	82	...	...	...	...	...	99	99	82	...	99	99	88	98
9....	99	98	80	...	97	98	82	98	97	98	81	97	78	...	...	...	...	98	98	98	80	98	98	98	86	97
8....	98	98	77	98	96	98	78	98	96	98	79	97	76	98	...	99	...	96	97	98	77	97	97	98	83	96
7....	98	97	75	96	96	97	76	96	95	97	76	96	72	94	99	98	...	93	96	97	74	96	96	97	80	94
6....	97	96	72	95	94	96	72	94	94	96	72	94	68	91	98	98	...	89	94	95	70	95	94	96	76	92
5....	96	95	69	93	91	95	68	93	92	95	68	93	64	86	98	96	...	83	92	94	66	93	92	93	71	90
4....	94	94	65	90	90	93	64	90	90	94	63	90	59	78	96	94	...	74	88	92	60	90	89	90	65	87
3....	91	90	60	86	86	90	58	86	88	91	56	87	52	67	92	91	98	61	82	88	54	87	85	86	59	83
2....	85	86	54	80	81	84	52	82	82	85	48	82	45	52	82	80	94	43	75	84	47	82	80	80	51	77
1....	74	74	44	69	70	72	40	70	70	75	40	70	36	30	58	50	77	25	62	75	38	70	70	70	40	68
0.5..	61	56	36	55	56	54	32	57	58	60	33	58	30	20	34	24	45	18	50	61	32	57	57	57	32	57
0.25.	50	38	28	43	41	35	26	45	48	44	30	43	27	13	22	15	23	16	40	44	27	44	48	41	27	46
0....	47	19	24	31	27	20	18	27	36	28	22	28	23	08	12	12	13	15	33	29	25	32	35	31	24	35

Δλ	H10				H11				H12				H13		H14		H15	H16	H17
	a	b	c	d	a	b	c	d	a	b	c	d	b	c	b	c	b	b	b
20....	...	...	...	...	...	...	...	...	...	...	...	...	...	...	...	...	...	...	...
15....	...	...	...	...	...	...	...	...	...	...	...	...	...	...	...	...	...	...	...
10....	99	99	93	...	...	...	95	...	...	...	...	...	...	...	...	...	...	...	...
9....	99	99	91	...	...	99	94	...	...	...	...	...	...	...	...	...	...	...	...
8....	98	98	88	...	...	98	92	...	...	...	...	...	...	...	...	...	...	...	...
7....	97	97	84	...	...	98	88	...	...	...	...	...	...	...	...	...	...	...	...
6....	96	96	80	...	99	97	85	...	99	...	94	...	99	...	...	...	...	...	...
5....	95	95	75	97	98	96	80	97	98	...	88	...	98	97	99	...	...	...	...
4....	93	92	69	94	96	95	74	95	96	96	82	97	96	92	98	96	...	...	...
3....	90	90	62	90	91	92	66	92	94	93	75	93	94	84	96	90	98	99	98
2....	84	85	52	85	86	87	56	86	88	89	66	86	91	72	93	78	95	98	96
1....	71	71	41	74	76	74	46	76	75	78	49	73	80	54	84	59	88	90	91
0.5..	59	56	32	62	66	59	39	64	64	64	39	64	66	45	72	49	80	82	84
0.25.	47	42	28	52	57	43	36	54	59	52	36	61	57	41	58	44	70	75	78
0....	40	33	26	46	46	37	34	46	57	45	35	59	52	38	54	41	59	70	77

The present hydrogen-line profiles are systematically narrower than those found by Chamberlain and Aller (1951). Consequently, we may expect even lower surface gravities and temperatures than those found in the earlier work. The weaker metallic lines invariably possess a needle-sharp appearance, indicating that the influence of rotation or turbulence is negligible; their true profiles cannot be measured with present spectroscopic equipment. Theoretical discussion has therefore been based on the equivalent widths. For hydrogen lines, however, the experimental data are more than sufficient for the present level of theoretical analysis. The lines have deep, relatively sharp cores and

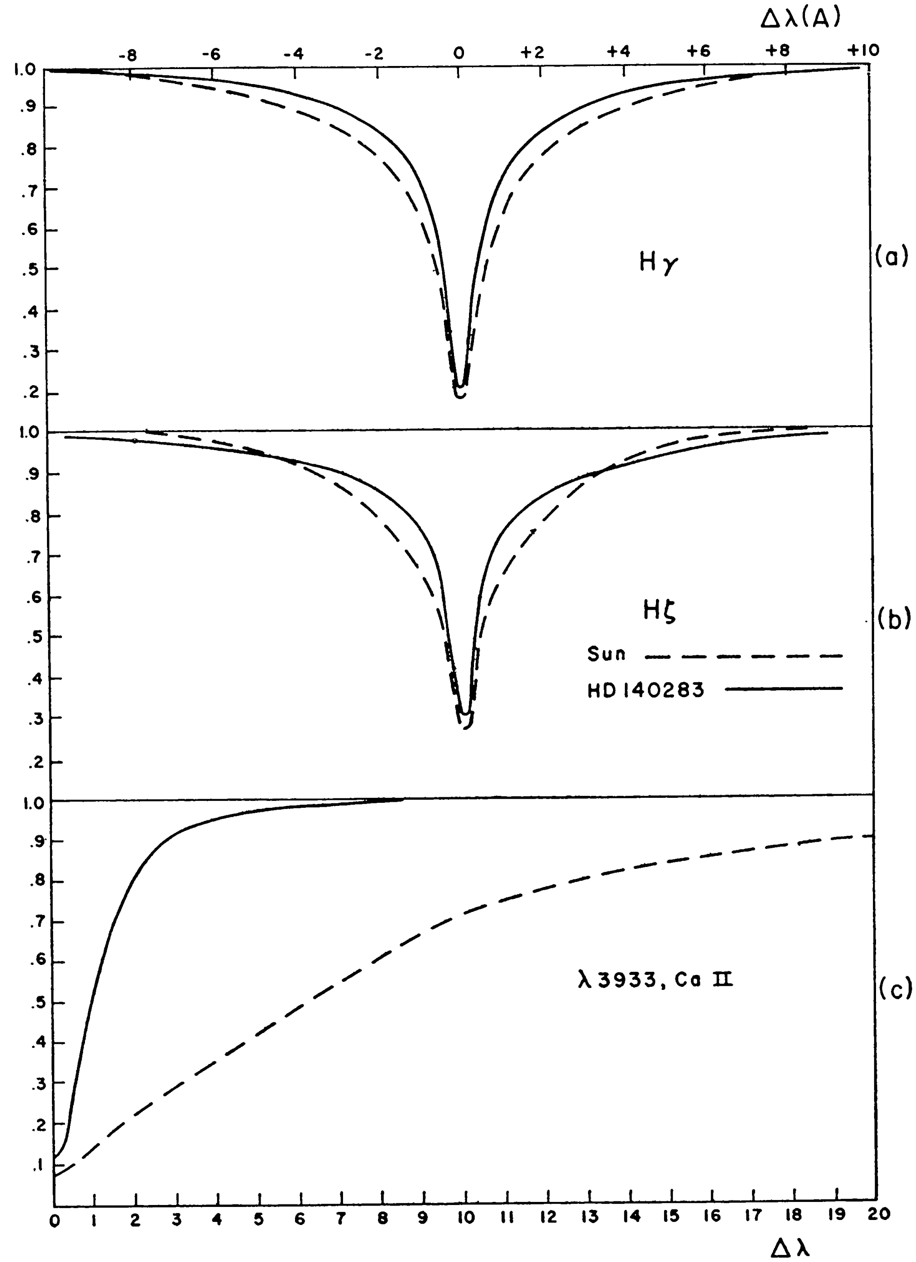

FIG. 7.—(*a*, *b*) Comparison of the hydrogen-line profiles in HD 140283 with those at the center of the solar disk. (*c*) The reflected mean profile of λ 3933 of Ca II compared with the line in the integrated spectrum of the sun.

broad, shallow wings; they need not be corrected for instrumental broadening. Although these stars have nearly the same temperature as the sun and slightly lower electron pressure, the hydrogen lines can be traced to much higher principal quantum numbers, partly because of the weaker ultraviolet metallic lines.

Figure 7 contains a comparison of some profiles in the subdwarf HD 140283 with those in the sun. The near-equality of the residual central intensity shows that the temperatures are nearly the same. The hydrogen-line cores are extremely sharp, a general feature of halo–population II spectra from subdwarfs to globular-cluster giants. The sharpness and weakness of λ 3933 indicate the abundance deficiency of Ca II. For example, at residual intensity 0.90, the width of the line in the sun is ten times that in the subdwarf, an abundance ratio of 100 for equal damping constants.

Although we lack a proper set of subdwarf models for different surface gravities and temperatures, we shall compute the profile of Hγ on the basis of the Griem and Kolb (1959) theory of hydrogen-line broadening. At large distances from the center of the line, the electronic effects dominate over ionic effects, except at the higher electron densities. The steep variation in line to continuous absorption coefficient with optical depth makes it impossible to predict meaningful profiles by a single choice of T and P_e. We have therefore used the subdwarf model by Swihart (1956), even though his value of log A = 5.0 is too small. We have extended his model to larger τ by assuming that $T(\tau)$ varies in accordance with the usual gray-body distribution at large τ. We include the following sources of lines broadening: (1) Doppler broadening, (2) natural damping, (3) van der Waals interaction, (4) resonance broadening, and (5) Stark broadening.

The natural damping of Hγ is determined almost entirely by the lifetime of the lower level, which consists of a 2s and a 2p term,

$$\Gamma_{2s,\,2p} = \frac{1}{\Sigma\varpi_i}\,\Sigma\varpi_i A_i = 4.68 \times 10^8\ \mathrm{sec}^{-1}\,, \tag{17}$$

and the total radiative damping, Γ_{rad}, is

$$\Gamma_{\mathrm{rad}} = \Gamma_{2s,\,2p} + \Gamma_{2s,\,2p} = 4.85 \times 10^8\ \mathrm{sec}^{-1}\,. \tag{18}$$

The van der Waals interaction is found in Aller (1953, chap. 8, eqs. [8], [9], [17], [19]). If we adopt $\bar{T}$ = 5800° K, the radius is ρ_0 = 4.17 A, and

$$\Gamma_{VW} = 79\,\frac{V}{T}\,P_g\,. \tag{19}$$

Here V is the mean relative speed of two hydrogen atoms, and P_g is the total pressure, in this case largely that of neutral hydrogen. The resonance broadening is given by Γ_{ν_0},

$$\Gamma_{\nu_0} = \frac{4\,e^2}{3\,m\nu_0}\,f_{nn'}\,N\,, \tag{20}$$

with ν_0 the frequency of the resonance line and f its oscillator strength (Breen 1957). For our purposes we need consider only the lower level, since $f_{12} \gg f_{15}$. Insertion of numerical values gives, for Hγ,

$$\Gamma_{\nu_0} = 4.16 \times 10^8\,\frac{P_g}{T}\,. \tag{21}$$

Finally, the total damping constant from these three causes is given by $\Gamma_{\mathrm{rad}} + \Gamma_{VW} + \Gamma_{\nu_0} = \Gamma$. From Aller (1953, p. 334) we obtain the total contribution to the absorption coefficient by these causes as

$$a_\lambda = 16.5 \times 10^{-26} f_{\mathrm{H}\gamma}\,\frac{\Gamma}{\gamma_{cl}}\left(\frac{\lambda_0}{\lambda - \lambda_0}\right)^2, \tag{22}$$

with γ_{cl} the classical radiation damping constant. The result, numerically, with $\Delta\lambda$ the distance from the center of the line in A, $f = 0.0447$, is

$$a_{\lambda} = 0.00139 \times 10^{-16} \frac{1}{(\Delta\lambda)^{2}} \frac{\Gamma}{\gamma_{cl}}. \tag{23}$$

The value of $\Gamma/\gamma_{cl} \gg 1$ throughout the atmosphere, partly because of the collisional effects and partly because we have a subordinate line.

The Stark broadening, for Hγ, is

$$a_{\lambda} = 143.1 \times 10^{-16} \frac{P_e}{T} \left[\frac{1}{(\Delta\lambda)^{5/2}} + \frac{R}{(\Delta\lambda)^{2}} \right], \tag{24}$$

where R is obtainable from the work of Kolb and Griem. Table 12 gives data necessary

TABLE 12

DATA FOR CALCULATION OF Hγ LINE-BROADENING COEFFICIENT IN SWIHART'S SUBDWARF G-TYPE MODEL ATMOSPHERE

τ_0 (1)	τ_{4340} (2)	P_e (3)	P_g $\times 10^{-4}$ (4)	$\theta = 5040/T$ (5)	$\times 10^{-8}$ Γ_ν (6)	Γ_{VW} (7)	Γ (8)	Γ/γ_{cl} (9)	LOG $N_{0,2}$ (10)	k_ν (11)	R (12)	$\times 10^{16}$ A (13)	B (14)
0.05.....	0.045	2.34	2.95	0.930	22.7	0.65	28	24	14.78	0.057	1.20	0.0617	0.107
0.10.....	0.090	4.07	4.27	.907	32	0.94	38	32	15.03	0.088	1.15	0.1055	0.165
0.21.....	0.19	8.90	5.90	.871	43	1.27	49	42	15.38	0.161	1.00	0.223	0.281
0.43.....	0.39	23.5	7.58	.819	51	1.57	57.6	49	15.92	0.341	0.95	0.546	0.585
1.08.....	0.97	129	9.34	.726	56	1.82	62.6	53	16.90	1.135	0.75	2.67	2.07
2.11.....	1.90	563	10.24	0.643	59.5	1.88	61.2	52	17.70	3.17	0.65	10.30	6.85

for the calculation of the Hγ line in Swihart's G-type model atmosphere. Columns 1, 3, 4, and 5 are taken directly from his paper. The optical depth as λ 4340 is $\tau_{\lambda} = 0.9\,\tau_0$, where τ_0 is the optical depth at λ 5050 (col. 2). Then, using the equations just derived, we evaluate the damping constant due to resonance broadening (col. 6), van der Waals interaction (col. 7), the total damping constant (col. 8), and the ratio Γ/γ_{cl}. Column 12 gives R, the correction factor obtained from an extrapolation of the Kolb-Griem data to lower temperatures; the last columns give the corresponding values of A and B. Columns 10 and 11 give the population in the second level of hydrogen and k, the mean absorption coefficient, at the given optical depth. Since the important quantity is l_{ν}/k, where $l_{\nu} = N_{0,2}\, a_{\nu}$, we see that η increases very rapidly in the deeper layers of the star. The optical depth at a point ν in the line is computed from

$$dt_{\nu} = \left(1 + \frac{l_{\nu}}{k_{\nu}}\right) d\tau_{\nu}. \tag{25}$$

The residual intensity in the line is

$$r_{\nu} = \frac{F_{\nu}}{F_c}, \tag{26}$$

where F_{ν} and F_c are the emergent fluxes in the line and continuum:

$$\pi F_{\nu} = 2\pi \int_0^{\infty} B_{\nu}(t_{\nu}) E_{\nu}(t_{\nu})\, dt_{\nu}, \tag{27a}$$

$$\pi F_c = 2\pi \int_0^{\infty} B_{\nu}(\tau_{\nu}) E_{\nu}(\tau_{\nu})\, d\tau_{\nu}. \tag{27b}$$

The result is that the profiles computed by taking into account all the sources of line broadening differ by a negligible amount from those obtained using the pure Kolb-Griem theory. This can be seen from a comparison of equations (23) and (24), since, even with the low value of P_e/T and the large Γ/γ_{cl}, the numerical coefficient of the Stark broadening is large.

TABLE 13

PROFILE OF Hγ

$\Delta\lambda$	1 A	2.5 A	4 A	6 A	10 A	
r_ν	0.63	0.76	0.81	0.86	0.91	Theoretical
	0.72	0.87	0.92	0.95	0.98	Observed mean, HD 19445, 140283

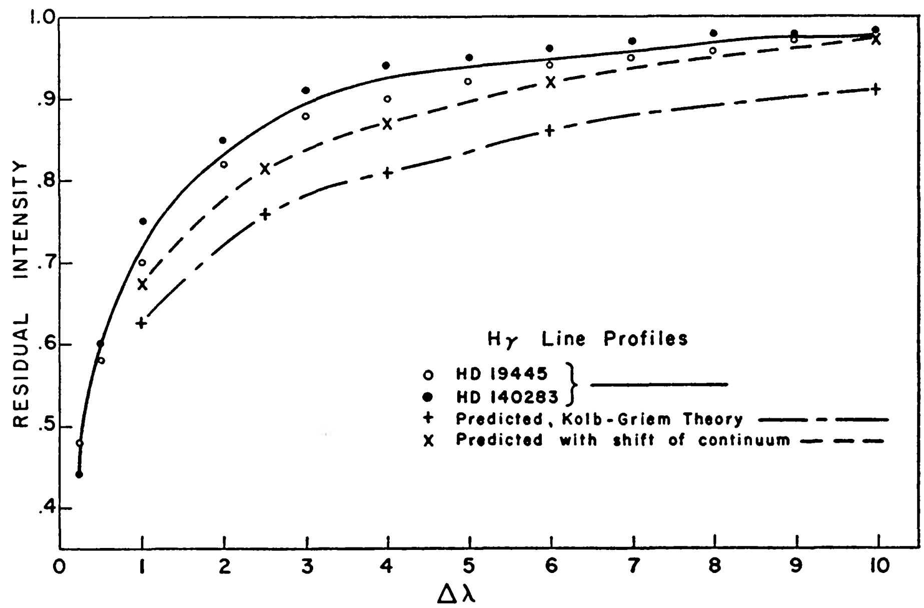

FIG. 8.—The observed profiles of Hγ in HD 19445 and HD 140283 are very similar. The Stark (and other) broadening sources, based on the Kolb-Griem theory, give the broad profile shown by the lowest, dashed curve. The observed profiles may have been drawn with respect to a continuum drawn too low because of the extended wings of the line. If we adjust the theoretical profile to coincide with that observed at $\Delta\lambda = 10$ A, the agreement is fairly good.

The actual profiles were calculated with slightly different values of B than those in Table 12, arising from a different mode of extrapolation of the Kolb and Griem coefficients to the layers significant in line formation. This difference has no influence on the final line profiles. Comparison with observation is given in Table 13.

The most striking feature of the theoretical calculation is the extreme extent and flatness of the line wings. If the theory is even approximately correct, we must conclude that we have greatly underestimated the extent of the wings on our tracings in the two best-observed subdwarfs. On the tracings, we used a continuum such that the wings merged with it at a finite slope about 10 A from the line center; the theoretical prediction is that at this point the line depth is still 9 per cent. Hence, if we wish to compare theory and observation and assume that an error of 9 per cent in the location of the continuum is possible, we should lower the observed and theoretical profiles to agree at $\Delta\lambda = 10$ A. We have done this in Figure 8 by adjusting the continuum. With such an adjustment, the theoretical profile is deeper than the observed—a reasonable effect, since the temperature of HD 140283 is much below that of the model which was assumed in computing the line profile. Physically, the great extent of the wings is to be understood as a consequence of the rapid increase in P_e at large τ, which broadens the line absorption coefficient, caused by the increasing ionization of hydrogen. A good portion of the continuous spectrum of the star is actually formed above the zone that makes the major contribution to the wing. Another consequence is that the wings of the higher members of the Balmer series must overlap, reducing $N_{0,\,2}$ deduced from weak lines. These effects should be investigated on tracings with a photoelectric scanner. We require, eventually,

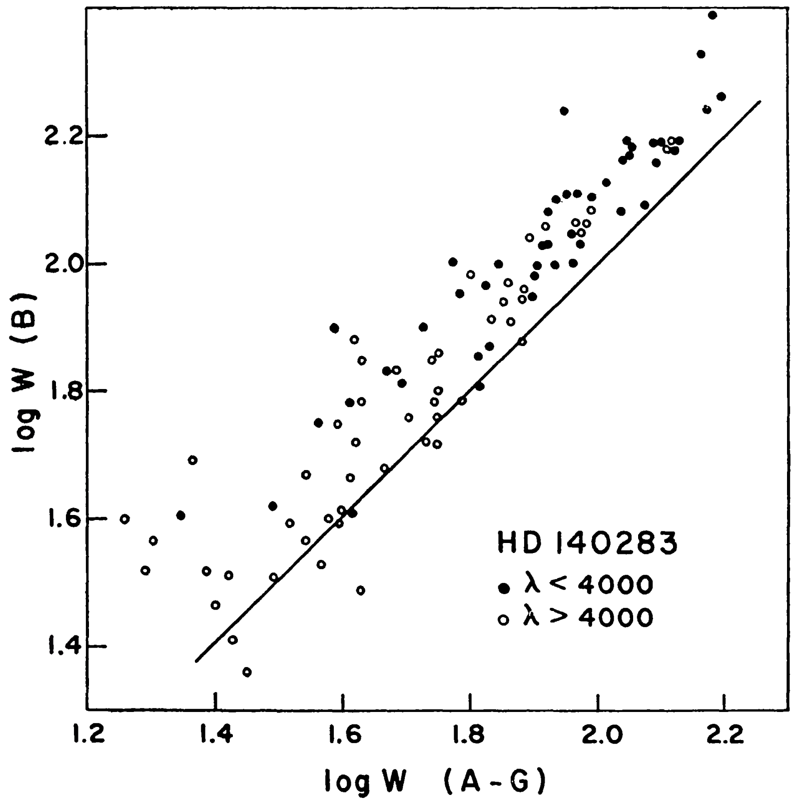

FIG. 9.—Comparison of logarithms of measured equivalent widths, by Baschek (*abscissa*) and by Aller and Greenstein (*ordinates*); W is in milliangstroms. The 45° line shows that there is a systematic difference in log W of about 0.10 and no significant dependence on wave length.

a family of model atmospheres for subdwarfs, so that the profiles of the hydrogen and Ca II lines may be computed over a wide range of temperatures, hydrogen/metal ratios, and surface gravities.

Inspection of Figure 8 might suggest that the greater strength and width of the predicted Hγ line could also arise from departures from local thermodynamic equilibrium. If we are not allowed to raise the "observed" continuum level, we could say that $N_{0,\,2}$ is reduced by a factor of about 4 near $\Delta\lambda = 2$ A, and by an even larger factor in the extreme wings. The sense of the required variation of $N_{0,\,2}$ with $\Delta\lambda$ is incorrect, however, for deviations from local thermodynamic equilibrium, which should be largest at small τ and therefore at small $\Delta\lambda$.

The actual last Balmer line clearly visible in HD 140283 is H20, which has a shallow core severely blended with metallic lines; higher members of the series may still be present. Application of the Inglis-Teller formula gives $\log N_e \leq 13.51$, or $\log P_e = +1.39$, in contrast with our $\log P_e = +0.34$ determined from the ionization of the metallic lines. Note that, in Table 12, log $P_e = +1.39$ occurs at $\tau = 0.5$, while log $P_e = +0.34$ occurs near $\tau = 0.05$. Such differences in level of formation are not unexpected but indicate the need for further work involving model atmospheres.

ADDENDUM: HD 140283

After this paper was completed, Baschek (1959) published the results of his analysis of HD 140283 based on Mount Wilson spectra taken by Unsöld at 10 A/mm. It would be difficult now to revise the present computations on the basis of his model atmosphere. In addition, most of his data are for the near ultraviolet and, because of lower dispersion, refer to fewer elements. Some major points of difference and agreement should be mentioned.

1. In Figure 9 we compare the measured equivalent widths, which differ systematically in the sense that log W (Baschek) − log W (Aller-Greenstein) = +0.10. A difference of 25 per cent is quite common between two different investigations of the same star. The lower dispersion probably tends to increase W; habits of drawing lines and continuum may easily account for the full amount. It is clear that below W = 50 mA, the

TABLE 14

	Star		Sun		$\langle [N]_{A,G} \rangle - \langle [N]_B \rangle$
	θ_e	log P_e	θ_e	log P_e	
A and G...........	0.92	0.34	0.89	1.30	−0.12±0.07
Baschek rough*.....	.91	.91	0.89	1.51	
Baschek model......	0.85	0.20*	....	....	−0.36±0.07

* Log P_e evaluated at $\tau = 0.10$.

differences are very large and predominantly positive, in the sense that Bashek measures many weak lines too strong. A statistical error in this sense is to be expected; lines that are marginally visible at lower dispersion are statistically too strong, since no one measures negative equivalent widths. The correlation is the same in the ultraviolet as in the blue, showing that no important error depends on wave length.

2. Baschek used an effective temperature $T_e = 5940°$, based on unpublished six-color photometry of Stebbins and Kron and the color-temperature calibration by Stebbins and Whitford (1945). Old values of the blanketing correction for the sun were used. The calibration of the six-color scale, by the solar T_e, is difficult. Our value of T_e, 5450°, is based on a more elaborate calibration of the absolute fluxes by Code (1959), together with the line blanketing and approximate models by Melbourne (1959). Since our method is more precise and since T_e enters critically into the abundances, as derived from neutral atoms, the lower T_e we used is particularly important.

3. The abundances derived from the rough analysis agree systematically with those of Baschek. The method of analysis is completely different; we used solar η_0's, and Baschek used laboratory gf-values with normalization to absolute. The lines are different, his work being largely in the ultraviolet. Some of the stratification in the level of formation of lines, involved in the model-atmosphere approach, is canceled out by our differential method, comparing sun and star. A comparison of the results is given in Table 14. Approximate weighting factors were used in forming the mean difference of the logarithm of the abundance ratios, sun/star, as determined by us $\langle [N]_{A,G} \rangle$ and by Baschek $\langle [N]_B \rangle$. His abundance deficiency is 30 per cent greater than ours, in the rough analysis, and 2.3 times greater if the model-atmosphere method is used. If we can assume that the model-atmosphere analysis results in an increase in abundance deficiency

of 0.24 in the logarithm, we can apply such a correction to our solution, with more accurate data and a different T_e, in our rough analysis. In that case the weighted mean deficiency of the metals is log $A^{\odot}/A^* = +2.22$.

4. Baschek finds an extremely high abundance of Ni, nearly equal to that of Fe. We found an increase in the Ni/Fe ratio between HD 140283 and the sun by a factor of 4. Although we agree on the high relative stellar abundance of Ni, Baschek also asserts that a renormalization of laboratory *gf*-values results in Ni/Fe ≈ 1 in the sun. This surprising result needs much more proof before it can be accepted; a discussion is contained in Goldberg, Müller, and Aller (1960), where the absolute *f*-value of Ni is treated.

5. The model atmosphere should give improved profiles for the Balmer lines. Baschek used only the Holtsmark broadening theory, which gives a narrower predicted line than does the Kolb-Griem theory. His observed line profiles agree well with ours, in that he finds a line depth at $\Delta\lambda = 5$ A of 8 per cent for Hγ, where we find 5 per cent. Thus an improved line-broadening theory applied to his model would result in the observed line being narrower than would be predicted—the same discrepancy that we found.

6. The accuracy of our observational data, especially when averaged over the three G-type subdwarfs, is greater, so that the small differential abundance changes found in our Table 10 retain the degree of reliability given in our text.

Code (1959) has published the results of a study of the energy distribution in subdwarfs. His earlier work has been put on an absolute-flux basis; spectral scans of HD 19445 and HD 140283 were used. Combining these with the six-color measures of Stebbins and Whitford, he concludes that the apparent infrared excess gives, in fact, a real measure of the lower effective temperature of these stars, as compared with main-sequence stars of similar apparent spectral type. The effective temperatures are as follows: Code: 6000° for HD 19445; 5500° for HD 140283. Melbourne (adopted this investigation): 5800° for HD 19445; 5450° for HD 140283. Since Melbourne's investigation included a more elaborate study of line blanketing, the agreement may be viewed as excellent. These subdwarfs are, in fact, early and middle G stars, with extremely weak lines.

REFERENCES

Allen, C. W. 1955, *Astrophysical Quantities* (London: Athlone Press).
Aller, L. H. 1953, *Atmospheres of the Sun and Stars* (New York: Ronald Press).
Babcock, H. W. 1958, *Ap. J. Suppl.*, **3**, 141.
Baschek, B. 1959, *Zs. f. Ap.*, **48**, 95.
Bonsack, W. K., *et al.* 1957, *Ap. J.*, **125**, 139.
Burbidge, E. M., Burbidge, G. R., Fowler, W. A., and Hoyle, F. 1957, *Rev. Mod. Phys.*, **29**, 547.
Burbidge, G. R., and Burbidge, E. M. 1956, *Ap. J.*, **124**, 116.
Breene, R. G. 1957, *Rev, Mod. Phys.*, **29**, 94.
Chamberlain, J. W., and Aller, L. H. 1951, *Ap. J.*, **114**, 52.
Chandrasekhar, S. 1936, *M.N.*, **96**, 21.
Code, A. D. 1959, *Ap. J.*, **130**, 473.
Fowler, W. A., and Greenstein, J. L. 1956, *Proc. Nat. Acad. Sci.*, **42**, 173.
Goldberg, L., Müller, E. A., and Aller, L. H. 1960, in press.
Greenstein, J. L. 1954, *Les Processus nucléaires dans les astres* (Mém. Soc. R. Sci. Liège), **14**, 307.
———. 1956, *Proc. Third Berkeley Symposium* (Berkeley: University of California Press), **3**, 11.
King, R. B. 1948, *Ap. J.*, **108**, 87.
King, R. B., and King, A. S. 1938, *Ap. J.*, **87**, 24.
Griem, H. R., Kolb, A. C., and Shen, K. Y. 1959, *Phys Rev.*, **116**, 4.
Melbourne, W. G. 1959, thesis, California Institute of Technology. Results kindly communicated in advance of publication.
Michard, R. 1950, *Bull. Astr. Inst. Netherlands*, **11**, 227.
Parenago, P. P. 1958, *Astr. J. U.S.S.R.*, **35**, 169.
Pecker, J.-C., and Peuchot, M. 1954, *Mém. Soc. R. Sci. Liège*, **18**, 352.
Roman, N. G. 1955, *Ap. J. Suppl.*, **2**, 195.
Schwarzschild, M., Howard, R., and Searle, L. 1955, *Ap. J.*, **122**, 353.
Stebbins, J., and Whitford, A. E. 1945, *Ap. J.*, **102**, 318.
Swihart, T. L. 1956, *Ap. J.*, **123**, 151.
Unsöld, A. 1948, *Zs. f. Ap.*, **24**, 323.
Wrubel, M. H. 1949, *Ap. J.*, **109**, 66.